Resuscitation of Bacterial Biofilm by Sunlight: Effects on Different Enteropathogenic Bacteria

By:

Radia Shams Pritha

Student ID: 18136036

Faria Rahman Jeba

Student ID: 18136037

A thesis submitted to the Department of Mathematics and Natural Sciences in partial fulfillment of the requirements for the degree of Bachelor of Science in Biotechnology

Department of Mathematics and Natural Sciences

BRAC University, Bangladesh

June 2022

Declaration

It is hereby declared that

1. The thesis submitted is our own original work while completing Bachelor of Science degree at BRAC University.

2. The thesis does not contain material previously published or written by a third party, except where this is appropriately cited through full and accurate referencing.

3. The thesis does not contain material which has been accepted, or submitted, for any other degree or diploma at a university or other institution.

4. We have acknowledged all main sources of help.

Student's Full Name & Signature:

Student Full Name	**Student Full Name**
Student ID	Student ID

Approval

The thesis titled “Resuscitation of Bacterial Biofilm by Sunlight: Effects on Vibrio cholerae, Shiga Toxin Producing Escherichia coli” submitted by

Radia Shams Pritha (18136036),

Faria Rahman Jeba (18136037),

has been accepted as satisfactory in partial fulfillment of the requirement for the degree of Bachelor in Biotechnology on

Examining Committee:

Supervisor:

(Member) _____

Iftekhar Bin Naser, PhD

Assistant Professor,

Department of Mathematics and Natural Sciences,

BRAC University

Program Coordinator:

(Member) _____

Iftekhar Bin Naser, PhD

Assistant Professor,

Department of Mathematics and Natural Sciences

BRAC University

_____

External Expert Examiner: Full Name

(Member) Designation, Department

Institution

Departmental Head:

(Chair)

_____

A F M Yusuf Haider, PhD

Chairman and Professor,

Department of Mathematics and Natural Sciences,

BRAC University.

Ethics Statement

This material is an original work, which has not been previously published elsewhere. It is my own research and analysis in a truthful and complete manner. The paper properly credits all the sources used (correct citation).

Abstract

There is significant evidence that suggests that bacteria go through various mobile and immobile phases during their lifetime. All these various phases, in turn, facilitate the pathogenic bacteria to cause and spread diseases during the seasonal outbreaks. These reversible mobile and immobile phases in bacteria are most evidently seen through the making and then the breaking out of biofilms. Many factors induce bacteria to enter a sessile state in the form of biofilms, while many cause them to break out those biofilms and become activated i.e, pathogenic. In this study, we focused on the effect of sunlight as a factor for the bacteria to break out of those biofilms and be resuscitated to cause diseases. Biofilms of a number of cholera strains and shiga toxin producing E.coli that cause diseases during the months of March to July were subjected to sunlight throughout the winter season (December to February) using four different phases, i.e., methods of data collection and its effects were observed and analyzed using appropriate statistical analysis. The resulting data and statistical analysis suggests that biofilms in the winter sunlight do not get resuscitated and a significant amount of planktonic bacteria does not come out of the biofilms to cause diseases. As a result, during the winter seasons, the incidence rate of some of the diseases may stay low as the causative bacteria in the waters stays immobile within the biofilm structures. However, in order to provide any conclusive evidence, round the year study including more samples is required.

Acknowledgement

First of all, we wish to declare our humble gratitude to Almighty Allah, who has bestowed the gift of utmost mercy, and given us the strength, patience and understanding required to complete this work amid this Covid- 19 situation.

We convey our special thanks to Professor A. F. M. Yusuf Haider, PhD, Chairman, Department of Mathematics and Natural Sciences, BRAC University, who always has tremendous support for every student. We express our gratitude to our supervisor, Dr.Iftekhar Bin Naser, PhD, Assistant Professor, Department of Mathematics and Natural Sciences, BRAC University, for his encouragement and continuous guidelines for this research. Additionally, we are grateful to Afia Nawshen, Lecturer, Department of Mathematics and Natural Sciences, BRAC University, for always guiding us and mentoring us throughout the project. We are indebted to all the extraordinary people of the Life Science Laboratories, BRAC University. Without their all-time support this would not be completed. We would like to specially recognize Asma Afzal, Lab Officer, and Tanzila, Nadira and Ashiq, Lab Assistants, Life Science Laboratories, BRAC University for being so patient and helpful towards us for the entirety of the project. We would also like to express our deepest respect to Mahboob Hossain, PhD, Professor, Department of Mathematics and Natural Sciences, BRAC University for always being a great inspiration.

We sincerely thank our beautiful family who trusted in us and are always there for us. This journey would be incomplete without some dear friends. Abida Nurun Nahar, Maisha Farzana, Anika Raiana, Sadia Zaman Shetu, Salwa Khair, Lamisa Shaik and our senior, Nishat Tasnim Ananna who were our greatest supporters while we did this work. We are very grateful and indebted to all of these people.

Sincerely,

Radia Shams Pritha,

Faria Rahman Jeba,

Department of Mathematics and Natural Sciences, BRAC University.

Table of Contents

List of Figures

List of Tables

Table **Page**

List of Acronyms

STEC- Shiga Toxin-Producing *E. coli*

EPS- Exo-Polysaccharide

VPS- *Vibrio* Polysaccharide

CVEC- Conditionally Viable Environmental Cell

VBNC- Viable But Not Culturable

OD- Optical Density

ELISA- Enzyme-Linked Immunosorbent Assay

EIA- Enzyme Immunoassay

RIA- Radial Immunoassay

ELISPOT- Enzyme Linked Immuno Spot Assay

HUS- Hemolytic Urine Syndrome

HC- Hemorrhagic Colitis

CTX- Cholera Toxin

ER- Endoplasmic Reticulum

AFR6- ADP ribosylation factor 6

c-AMP- Cyclic Adenosine Monophosphate

PKA- Phospho Kinase

CFTR- Cystic Fibrosis Transmembrane Receptor

LPS- Lipopolysaccharide

STX- Shiga Toxin

PP- Peyer's Patch

LB- Luria Broth

LA- Luria Bertani Agar

QS- Quorum sensing

CAI-1- Cholerae autoinducer-1

AI-2- Autoinducer-2

VPS- Vibrio Polysaccharide

HCD- High Cell Density

LCD- Low Cell Density

LSR- Lipolysis Stimulated Lipoprotein Receptor

HapR- Hemagglutinin Protease Regulatory Protein

aW- Water Activity

TCBS- Thiosulfate-citrate-bile salts-sucrose

TSI- Triple Sugar Iron

CBB G-250- Coomassie Brilliant Blue G-250

CFU- Colony Factor Unit

Chapter 1:

Introduction

1. Introduction

1.1 Background:

Bangladesh is a highly cholera-endemic country where cholera and diarrhea outbreaks are seen to increase in the summer season while it goes away during the winter season. Many factors cause these seasonal outbreaks and many factors have been investigated in order to validate this periodic increase and decreased infections caused by the causative agents of these diseases. Bacterial biofilms have been a topic of focus in order to explain this.

Toxigenic *Vibrio cholerae* persists in cholera-endemic areas mostly in a biofilm-associated condition, in which the bacteria are fixed in an exopolysaccharide matrix. Biofilm-associated cells frequently go dormant, forming conditionally viable environmental cells (CVEC), which are resistant to culture on standard bacteriological medium. However, by different methods, these cells can naturally revive into the active planktonic form, reproduce, and create cholera epidemics (Naser et al., 2017). Among these different methods, many of them like, irradiation, bacteriophage infection, chemical treatment etc. has been explored as possible candidates that resuscitates the cholera bacterial biofilms and releases the planktonic bacteria which then causes infections and in a larger scale, epidemics. However, sunlight is yet to be explored as one of the factors that resuscitates bacterial biofilms and causes seasonal outbreaks of cholera in Bangladesh.

According to the principle where cholera infections decrease during the winter season, it can be assumed that sunlight does not break bacterial biofilms in the winter season to release the planktonic bacteria which causes the infections as the sunlight is not very strong and does not stay for a long time in winter. As a result, infectious bacteria like Vibrio cholera and STEC remain dormant inside the biofilm structures unable to cause cholera and diarrhea respectively during the winter season.

1.2 Aim of the study:

The aim of this study is to investigate whether winter sunlight can resuscitate bacterial biofilms, releasing planktonic bacteria. Several diseases, like cholera, have seasonal outbreaks. If winter sunlight does not significantly degrade bacterial biofilm, this could explain the absence of outbreaks in winter, in contrast to summer.

Chapter 2:

Literature Review

2.1.1 Biofilms:

Many bacteria create a structured layer of protective encasement, called a biofilm that adheres microorganisms within and is made up of a complex polymeric substances (EPS) matrix. This is done in response to stress or some adverse environmental effect so that the bacteria can survive even in these situations. The production of a biofilm is a developmental process in which an auto-inducer which is a quorum sensing signal molecule, induces the secretion of EPS and results in the construction of a distinctive three-dimensional biofilm architecture. Biofilm development may be thought of as a survival mechanism for bacteria since it protects them against hazardous conditions like antibiotics, heat stress, and predation. A biofilm can include as many as $1.0x10^9$ cells per clump, which can be enough to contain an infectious dose of a disease in most circumstances (Huq et al., 2008). Evidence shows that pathogenic V. cholerae biofilm production aids the pathogen's persistence in the environment, where adhesion to surfaces in aquatic settings plays a critical part in the pathogen's epidemic cycles. Within biofilms, local microenvironments may be very varied, and organisms struggle for space under a variety of circumstances, including nutrition constraint, fluid movement, desiccation, toxic chemical gradients, and UV irradiation, and pH and temperature fluxes. As a result, biofilm development is a simple microbial survival strategy in which microorganisms, including pathogens, dwell in a dynamic equilibrium in which cell clusters grow, mature, and detach to spread to other surfaces (Hall-Stoodley & Stoodley, 2005). A biofilm three dimensional structure can be made up of one or more than one type of bacteria. They can be formed on both living and non-living surfaces and they can be found anywhere from lake water, raw food, sewage lines to kitchen sinks, animal teeth and laboratory tools. Commonly, biofilms are referred to as slime. However, inside this slime a unique and complex system develops that is stable and has a significant role in microbes' survival and pathogenesis.

2.1.2 Biofilm Development:

Biofilms are made up of proteins, polysaccharides, lipids, and DNA, and they form a protective matrix around bacteria, ensuring their integrity and survival. Microorganisms take up around 10% to 30% of the biofilm volume. Water makes up around 97 percent of the biofilm, and it is responsible for the flow of nutrients essential for bacterial life. As a preliminary stage in biofilm development, several microbes create clumps of planktonic/free cells in an aquatic environment. Attachment, cell-to-cell adhesion, expansion maturation, and dispersal are all processes in the biofilm formation process. Bacterial proliferation results in the formation of microcolonies, which

are encased in a hydrogel layer that serves as a barrier between the microbial population and the outside world. Within the bacterial community, cells interact with one another via quorum sensing (QS) systems, which use chemical signals to communicate. Communication is essential for the regulation of cellular processes, population density-based disease, and nutrition uptake, genetic material transfer between cells, motility, and secondary metabolite production. Parallel to the buildup of EPS, the biofilm grows. Lastly, detachment of bacterial strains from microcolonies is the final phase, which might result in the creation of a new biofilm colony in a different site (Preda & Săndulescu, 2019). And at one point of living inside a biofilm, bacteria can detach it and again come back to planktonic form. This depends on many internal or external factors. In this study it will be investigated if sunlight is one of them. The biofilm development cycle is shown in the figure below:

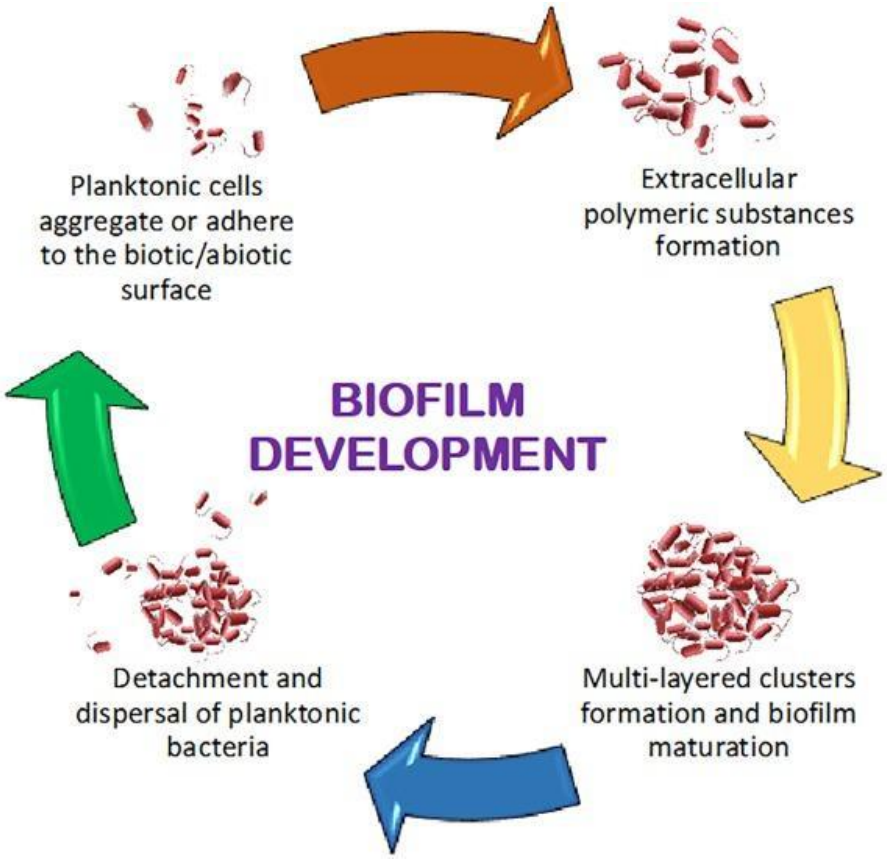

Figure 2.1: Biofilm development cycle (Preda & Săndulescu, 2019)

Biofilms form when bacteria in a given environment begin to interact and form bonds with one another. With time, this connection develops into cell clusters. These cell clusters are subsequently encased within the biofilm matrix.

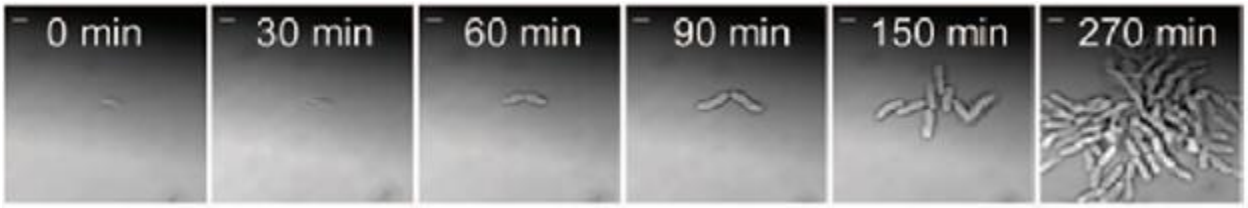

Figure 2.2: Vibrio cell cluster formation (Berk et al., 2012)

The cell clusters formed above are due to vibrio polysaccharide (VPS) secretion which acts like a "glue" or adhesive that attaches *V.cholerae* cells together over time as biofilm maturation occurs. This results in the formation of microcolonies composed of vibrio cell clusters.

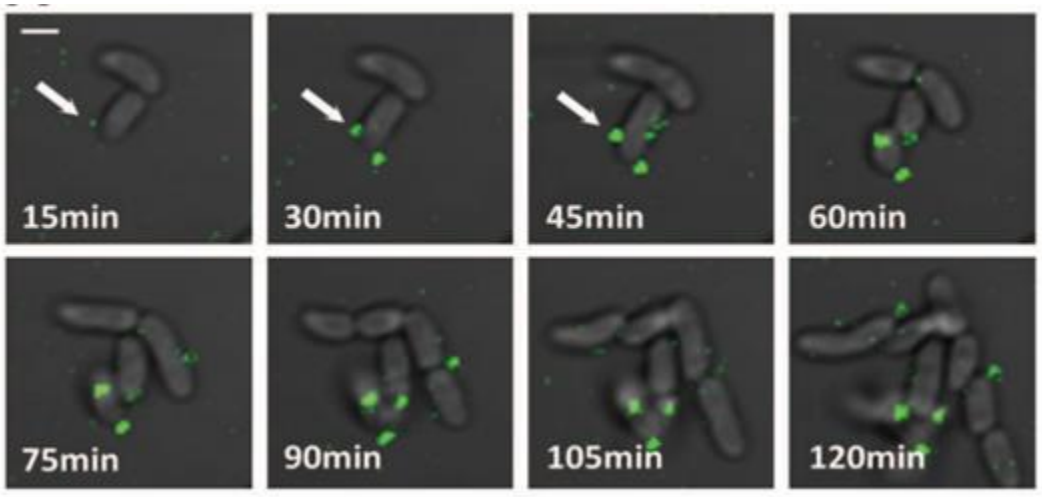

Figure 2.3: **Timelapse image of VPS secretion resulting in vibrio cell cluster**; the green dots represent VPS which is shown to increase in concentration over time (Berk et al., 2012)

In our experiment, we formed bacterial biofilm in solid surfaces like glass and plastic and the method how bacteria forms and adheres their biofilm to a solid surface is shown below:

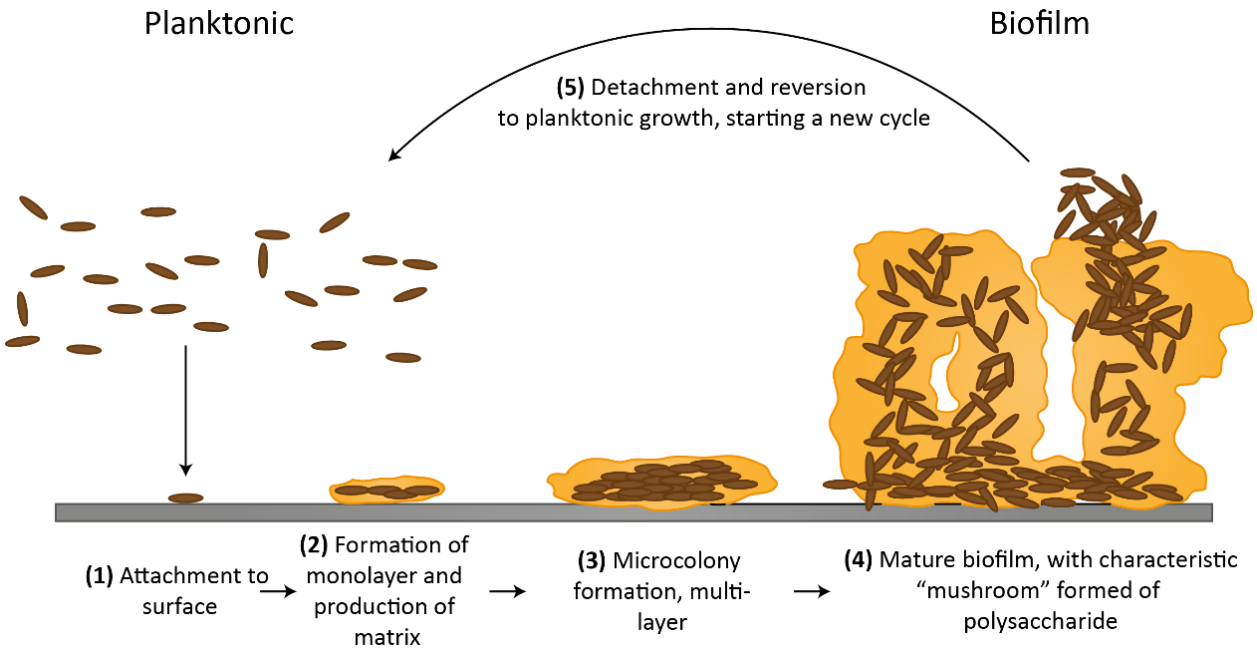

Figure 2.4: **Schematic representation of a biofilm formation on solid surface.** The formation begins with a reversible attachment of the planktonic cells represented by brown ovals, followed by the adhesion to the surface represented by gray (1). The bacteria then form a monolayer and irreversibly attach by producing an extracellular matrix (2). Next, a microcolony is formed where multilayers appear (3). During later stages, the biofilm is mature, forming characteristic "mushroom" structures due the polysaccharides (4). Finally, some cells start to detach and the biofilm, shown in yellow, will disperse (Hollmann et al., 2014)

2.2.1 Quorum Sensing and Autoinducers:

Quorum sensing (QS) is a bacterial communication mechanism that permits specialized activities like biofilm formation, virulence factor expression, secondary metabolite synthesis, and stress adaptation mechanisms like bacterial competition systems, including secretion systems (SS), to be regulated. It works by measuring cell density via chemical signals that allow bacteria to communicate with one another (Pena et al., 2019). As a result of this communication, the bacterial cells in a dense colony can control the gene regulation of each other. This bacterial gene regulation in response to cell density is performed through the production, release, and subsequent detection of extracellular signal molecules known as autoinducers. When the autoinducer concentration is

achieved, target gene expression is changed, allowing for behavioral changes that correspond to oscillations in cell population density. Some bacteria can detect and respond to various autoinducer signals, which might allow them to distinguish between species within a consortium in natural settings (Hammer & Bassler, 2003). Bacteria are thought to coordinate collective behaviors to complete tasks that would be hard for a single bacterium to complete alone and as a result, through quorum sensing all the bacteria in the community/colony communicates to collectively express the genes involved in making the biofilm structure which otherwise would not be possible for a single bacterial cell to make on its own.

2.2.2 Quorum Sensing and Biofilm Formation in *Vibrio cholerae:*

In Vibrio cholerae, several quorum-sensing circuits work in tandem to regulate virulence and biofilm development. Biofilm formation mainly depends on the high or low cell density as the reaction cascade depends on the availability of the autoinducers which are the cell signaling molecules. When QS autoinducers are unavailable, V. cholerae builds biofilms at low cell densities. When autoinducers concentration increases at high cell densities, biofilm formation is inhibited, and dispersion occurs. The two main autoinducers that are responsible for this relay operon system are cholerae autoinducer-1 (CAI-1) and autoinducer-1 (AI-2) whereas, CAI-1 is for intraspecies communication among Vibrio and is used to figure out Vibrio abundance, AI-2 is for interspecies communication as it is produced by a variety of bacterial species and it is presumed that V.cholerae uses the AI-2 system to assess the total bacterial cell density in the community (Hammer & Bassler, 2003). Both of these autoinducer systems converge the information they accumulate into a single and shared signal relay pathway that sets off a phosphorelay cascade (Bridges & Bassler, 2019). The CAI-1 system consists of the synthase CqsA which synthesizes the CAI-1 autoinducer and its subsequent sensor which is the CqsS, a two domain protein with the sensor domain and the histidine kinase domain. The sensor domain binds with the CAI-1 and the histidine kinase domain phosphorylates LuxO to set off the phosphorelay cascade leading to vpsA and vpsL gene and protein expression which forms the biofilm (Hammer & Bassler, 2003). VpsA and vpsL are part of vibriopolysaccharide (vps) gene clusters and these vps are essential for biofilm matrix formation in Vibrio cholerae (Fong et al., 2010). Simultaneously, there is the AI-2 system which consists of the LuxS synthase that synthesizes the AI-2 autoinducer and its subsequent sensor, LuxP/Q. The LuxP is a periplasmic binding protein which means it binds with the AI-2

signaling molecule and induces the LuxQ protein which also is a two domain protein where one sensor domain binds with the LuxP and the histidine kinase domain that phosphorylates the LuxO and starts the cascade reaction that ends at vpsA and vpsL gene expression and biofilm formation (Bridges & Bassler, 2019). The overall cascade reaction is shown in the illustration below:

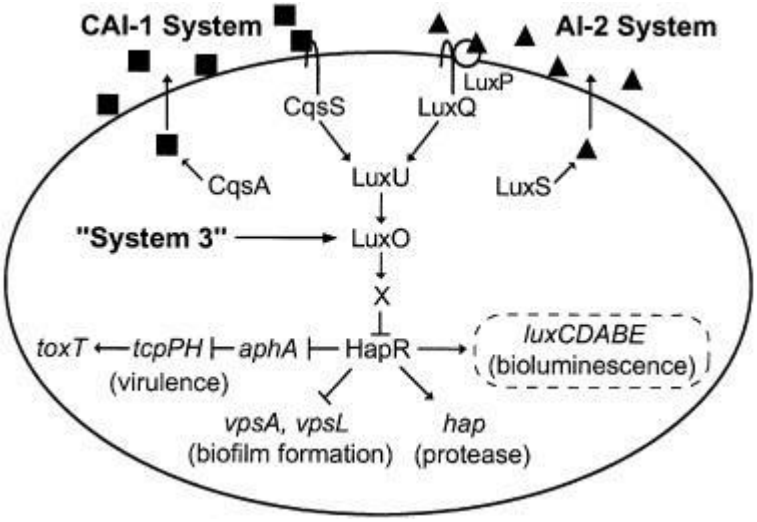

Figure 2.5: Lux operon containing CAI-1 and AI-2 systems involved in biofilm formation in V.cholerae due to quorum sensing (Hammer & Bassler, 2003)

As shown in the illustration above, the histidine kinase domain of the CqsS and LuxQ proteins phosphorylates LuxO protein via the phosphorylation of an integrator protein called the LuxU. The phosphorylated LuxO associates with σ^{54} and activates a repressor gene X. The repressor inhibits the transcription of hapR. HapR activates the production of hap protease while repressing the production of vpsA and vpsL and hence stopping biofilm production. This phosphorelay cascade depends entirely on the cell density ((Hammer & Bassler, 2003).

Low Cell Density (LCD):

Phosphate is transported from the CqsS and LuxP/Q sensors to the LuxU integrator protein at low cell density when autoinducer concentrations are low. The phosphate is transferred to LuxO via LuxU. Phospho–LuxO activates a putative repressor (X) that suppresses hapR expression when it interacts with σ^{54}. (the V. harveyi luxR homologue). HapR activates certain target genes while suppressing others. Biofilm development occurs at low cell density (i.e. when hapR expression is

suppressed), and V. cholerae produces aphA-dependent virulence genes that facilitates CT toxin production (Hammer & Bassler, 2003). This is illustrated in the figure below:

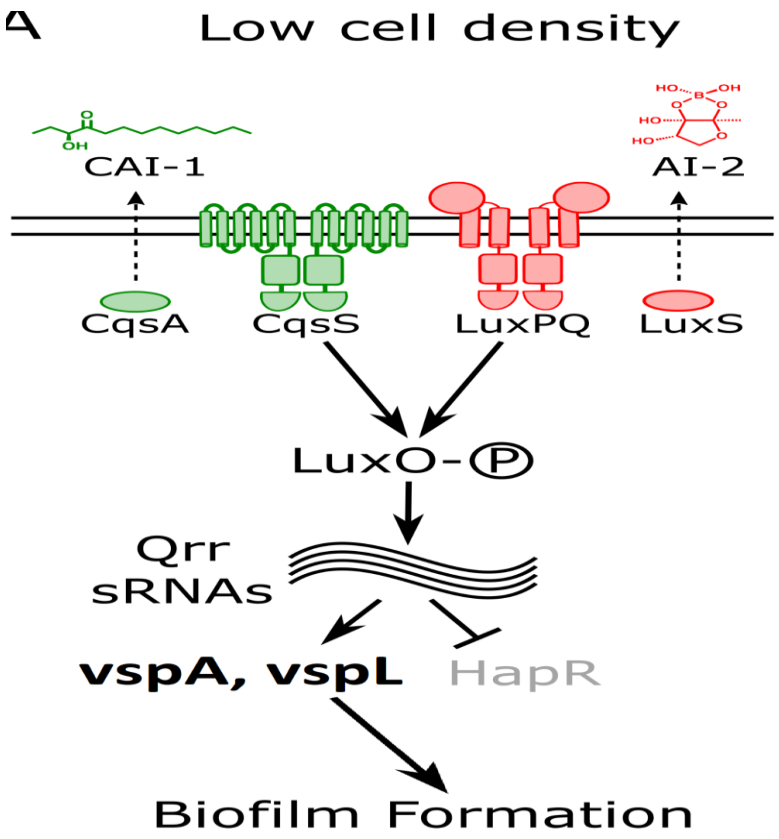

Figure 2.6: Lux operon cascade working at low cell density where hapR is repressed and vspA and vspL are activated so that biofilm is formed (Bridges & Bassler, 2019)

High Cell Density:

The flux of phosphate reverses at high cell density, resulting in LuxO dephosphorylation and inactivation. HapR is expressed, and via an unknown method, it represses the expression of vspA and vspL, which are biofilm formation genes, and stops virulence expression by binding to the aphA promoter and suppressing alphA transcription. HapR also activates the hap gene, resulting in the synthesis of HA/protease. The LuxO is not activated so vspA and vspL is also not activated (Hammer & Bassler 2003).

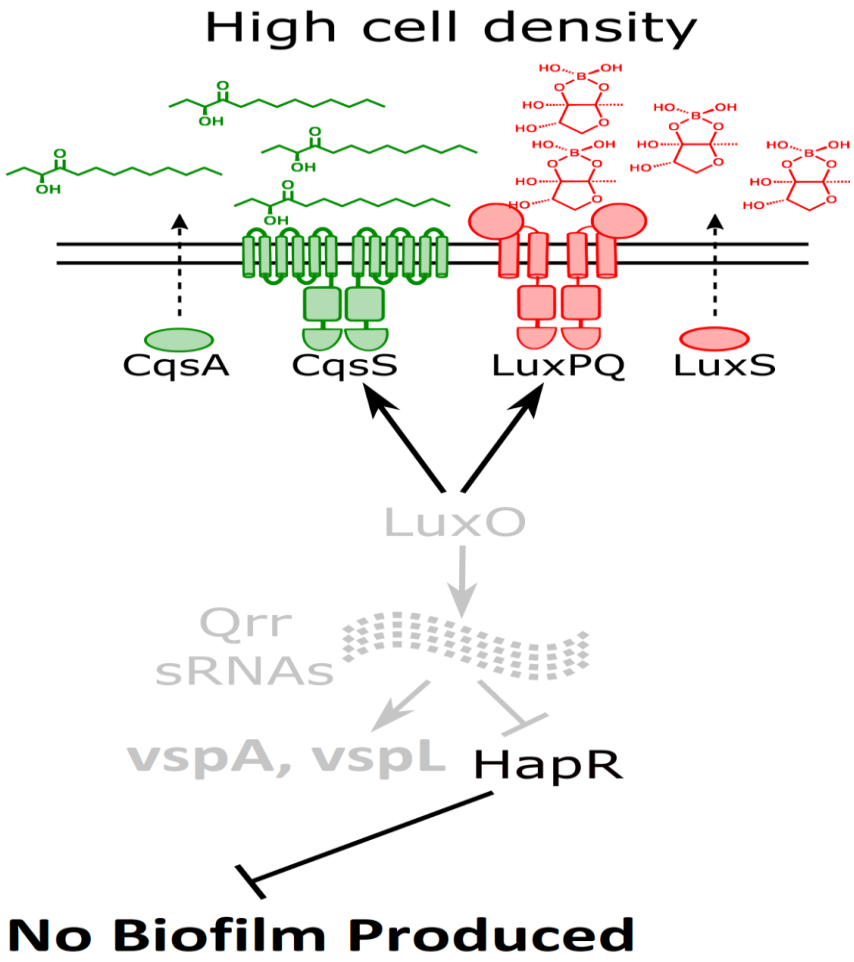

Figure 2.7: Lux operon cascade working at high cell density where HapR is not repressed while vspA and vspL is not activated so that biofilm is not produced (Bridges & Bassler, 2019)

2.2.3 Quorum Sensing and Biofilm Formation in *STEC*:

The regulatory network for the absorption of Escherichia coli autoinducer 2 (AI-2) is comprised of the LsrABCD transporter complex, its repressor, LsrR, and a cognate signal kinase, LsrK. The AI-2 quorum-sensing (QS) system relies heavily on this network. The whole phosphorelay cascade is part of the lsr operon where the lsr is lipolysis-stimulated lipoprotein receptor ("LSR - Lipolysis-stimulated lipoprotein receptor - Homo sapiens (Human) - LSR gene & protein", 2006). When cell density is high and AI-2 levels are low, fast uptake of AI-2 is not triggered. Many genes, including the lsr, flu, and wza genes, are binded and repressed by LsrR as LsrR is a repressor. As wza and

flu are biofilm forming proteins, no biofilm is formed during this time (Li et al., 2007). Wza is a lipoprotein and an essential part of the EPS that is the building blocks of E.coli biofilm (Dong et al., 2006) while flu is an autotransporter and a self-recognizing adhesin that is essential for biofilm formation in E.coli (Houdt, 2005). When AI-2 accumulates extracellularly during LCD, it is either delivered into cells via a non-Lsr route or accumulates within cells, where it binds to LsrR and derepresses several QS genes such as lsrR, flu, wza, and dsrA and biofilm is formed. Because phospho-AI-2 derepresses Lsr-mediated AI-2 uptake, it stays suppressed and no AI-2 is uptaken. Finally, when AI-2 concentrations hit the "threshold" for absorption and cells detect nutritional shortage, lsr imports AI-2 quickly. Following that, cells phosphorylate the imported AI-2 signal, causing LsrR/AI-2 regulation to stop and LsrR/phopho-AI-2 regulation to increase. As a result, a shift in the phosphorylation state of AI-2 and its binding to LsrR indicates a quick QS flip (Li et al., 2007). All this is illustrated in the figure below:

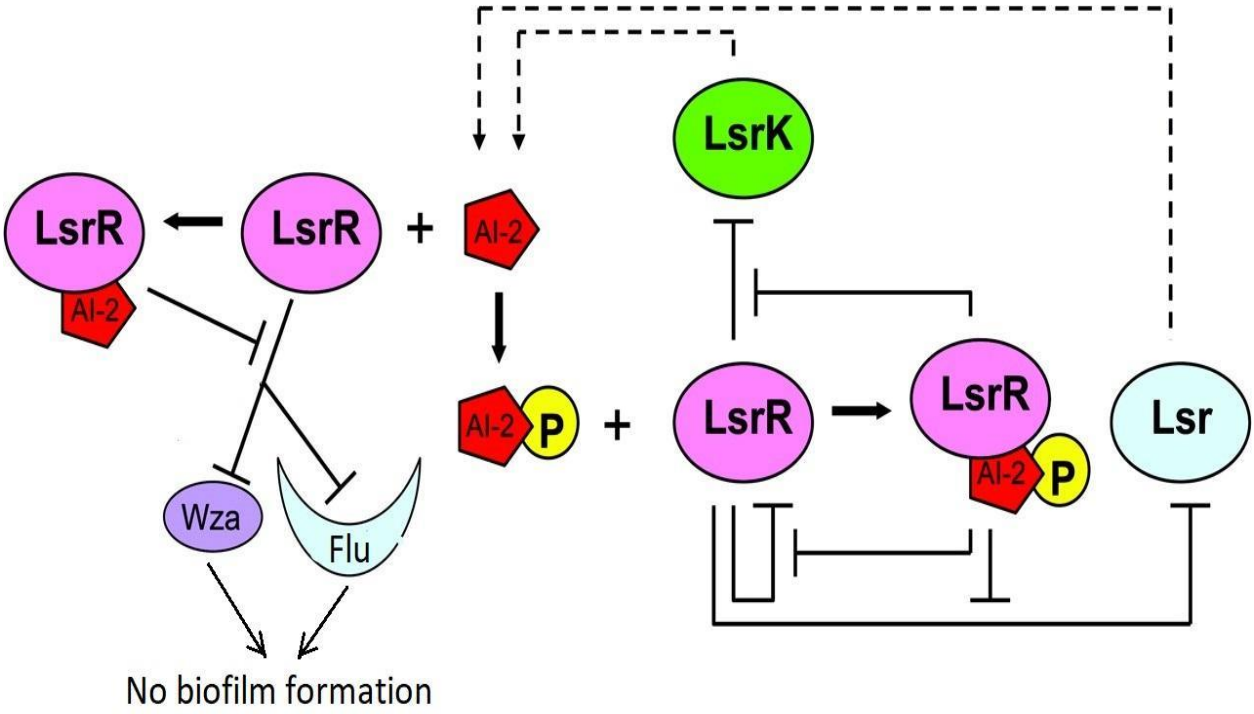

Figure 2.8: Lsr operon in E.coli quorum sensing resulting in Wza and Flu repression and no biofilm formation (Li et al., 2007)

2.4 Mutated *V.cholerae* Strains:

The *V.cholerae* strains used in this experiment are mutant strains “designed” specifically for elevated levels of biofilm formation for better distinguishability of its breakage due to sunlight. The strains were *V.cholerae 1712* which is a LuxO- mutant where the LuxO gene was inserted into an environmental *V.cholerae* strain that originally lacked this gene in the form of pLuxO (LuxO plasmid). On the other hand, another mutant strain of *V.cholerae* strain was used that was *V.cholerae 1877*. This strain is a HapR mutant strain where the HapR gene is permanently repressed in order to mimic a low cell density state so that the Lux operon keeps going on to make more VPS and hence more biofilm.

2.5 Pathogenic Significances of Biofilms:

According to the National Institutes of Health, biofilms are responsible for 80% of all human illnesses, and biofilms are now so common in the environment that they may be found everywhere from sewage treatment facilities to food processing plants to sensitive medical devices (Mosharraf et al., 2020). Biofilms are formed by many microorganisms that cause serious illnesses in humans. In fact, some of them must shift from sessile to motile in order to produce a serious illness. Vibrio cholerae has the ability to transition between motile and biofilm states. The understanding of the formation, control, and function of biofilms generated in the laboratory has increased dramatically in recent decades. Evidence shows that V. cholerae may form biofilm-like aggregates during infection, which may play a key role in disease pathogenesis and transmission. This bacterium's mobility helps it to reach and adhere to the infection's target spot and the biofilm state provides the required host resistance. In order to cause infection, the pathogen must colonize the human intestine, then spread throughout the body and be excreted. The virus travels throughout the human gut in this manner. When the pathogen binds to target cells, CT Toxin is injected into the intestinal cells, causing harm. Stools produced by patients include a combination of slime, cluster, and single cholera cells. (Silva & Benitez, 2016). As a result, the cholera bacteria is transmitted from person to person.

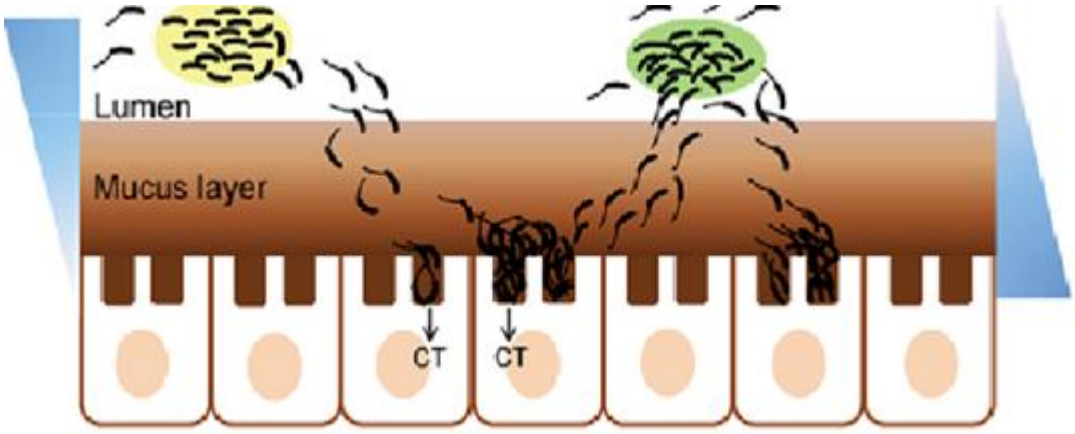

Figure 2.9: Transitions of vibrio cholera between sessile and motile form (Silva & Benitez, 2016).

STEC may create biofilms on a variety of surfaces often found in meat processing plants, including stainless steel, polystyrene, glass, polyurethane, and high-density polyethylene, in addition to generating biofilms under environmental conditions and on plants. The spread of STEC and contamination occurs when infected food is introduced into processing plants.

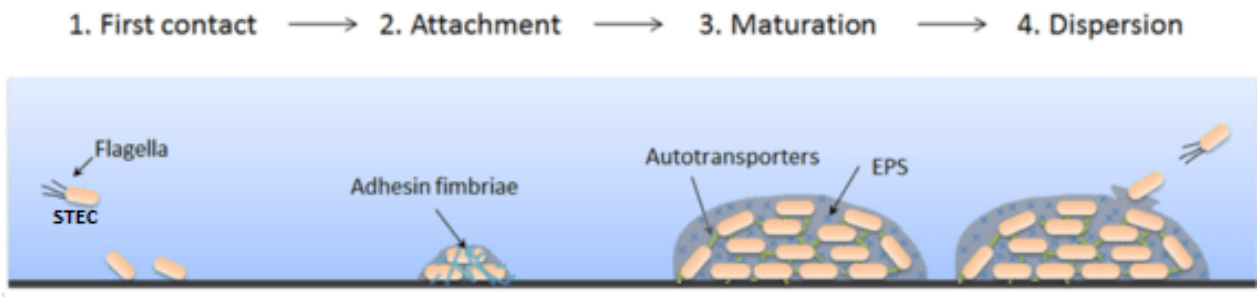

Figure 2.10: Schematic representation of biofilm formation in STEC on surfaces like solid environmental surfaces or gut linings (Vogeleer et al., 2014)

2.6.1 Diseases Caused by *V.cholerae*:

Vibrio cholerae causes the disease cholera in humans which is characterized by watery diarrhoea, vomiting and dehydration. There is a very specific pathway that cholera pathogenesis follows where the pathogen enters the human host through contaminated waters. *Vibrio cholerae* begins expressing virulence factors, such as cholera toxin, after reaching and inhabiting the target organ which is the small intestine. Cholera toxin is made up of two subunits, CtxA and CtxB, and the CtxB pentameric subunit binds to the ganglioside GM1 on the plasma membrane of the cell. The

cell subsequently consumes the GM1-bound cholera toxin, which is then transferred to the endoplasmic reticulum (ER). The CtxA and CtxB subunits then separate from one another. CtxA is a subunit of an enzyme. When released from the ER into the cytoplasm, ADP ribosylation factor 6 (ARF6) allosterically activates it. Adenylyl cyclase is activated by the ARF6-CtxA complex, which catalyzes a G protein-coupled receptor. This raises cAMP levels in the cell, causing the cystic fibrosis trans-membrane receptor to be phosphorylated (P) (CFTR). As a result, ions and water are effluxed into the small intestinal lumen, resulting in watery diarrhea (Baker-Austin 2018).

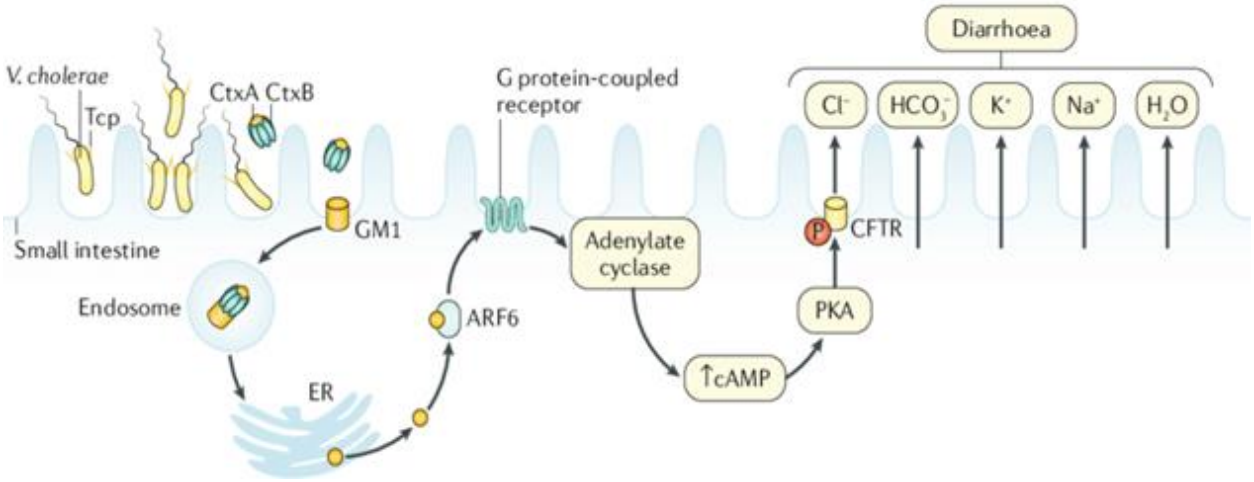

Figure 2.11: Cholera Pathogenesis (Baker-Austin, 2018)

2.6.2 Diseases Caused by *STEC*:

STEC (Shiga toxin-producing Escherichia coli) are foodborne bacteria that can cause serious damage to the intestinal mucosa and, in some circumstances, other internal organs of the human host following ingestion. The causative agent is E.coliO157. The adhering and effacing (A/E) lesions of enteropathogenic *E. coli* with the intimin gene (eae) and the fimbria of enteroaggregative E. coli are the most widely reported adherence systems. These organisms can cause enterohemorrhagic disorders like hemorrhagic colitis (HC) or the life-threatening condition hemolytic uremic syndrome by adhering to the intestinal lining and expressing Shiga toxin (HUS) (Nastasijevic et al., 2020). *STEC* infection symptoms include fever, diarrhea, and vomiting. The incubation period for this organism is 3 to 8 days, and most patients recover by 10 days. *STEC* may grow in temperatures ranging from 7°C to 50°C, with a preferred temperature of 37°C. However, the range can increase if the bacteria is in its biofilm state, in which case they can survive

below 7°C and above 50°C. *STEC* may develop in meals with a minimum water activity (aW) of 0.95 and in foods with an acidic pH of 4.4. It is killed by thoroughly boiling meals until all sections reach 70°C or above. Although *E. coli* O157:H7 is the most common *STEC* serotype in public health, other serotypes have been implicated in sporadic cases and outbreaks ("E. coli", 2018). Additionally, when *STEC* is in their mobile biofilm state, they are less sensitive to sanitizers and disinfectants, making it more difficult to kill (Vogeleer et al., 2014). The bacteria may bind to the terminal ileum and the follicle-associated epithelium of Peyer's patches after ingestion. Quorum sensing and activation by the host hormonal response, which includes adrenaline and norepinephrine, which are likely released during hemorrhagic colitis, help colonization. Shiga toxin attaches to the Paneth cell's globotriaosylceramide Gb3 receptor and travels through the intestinal epithelium. The toxin has been demonstrated to cause dysentery and apoptosis in the intestine. The inflammatory host response in the intestine is critical for bacterial clearance from the gut. Reduced intestinal response increases bacterial load, allowing more bacterial virulence factors to circulate (Karpman, 2012).

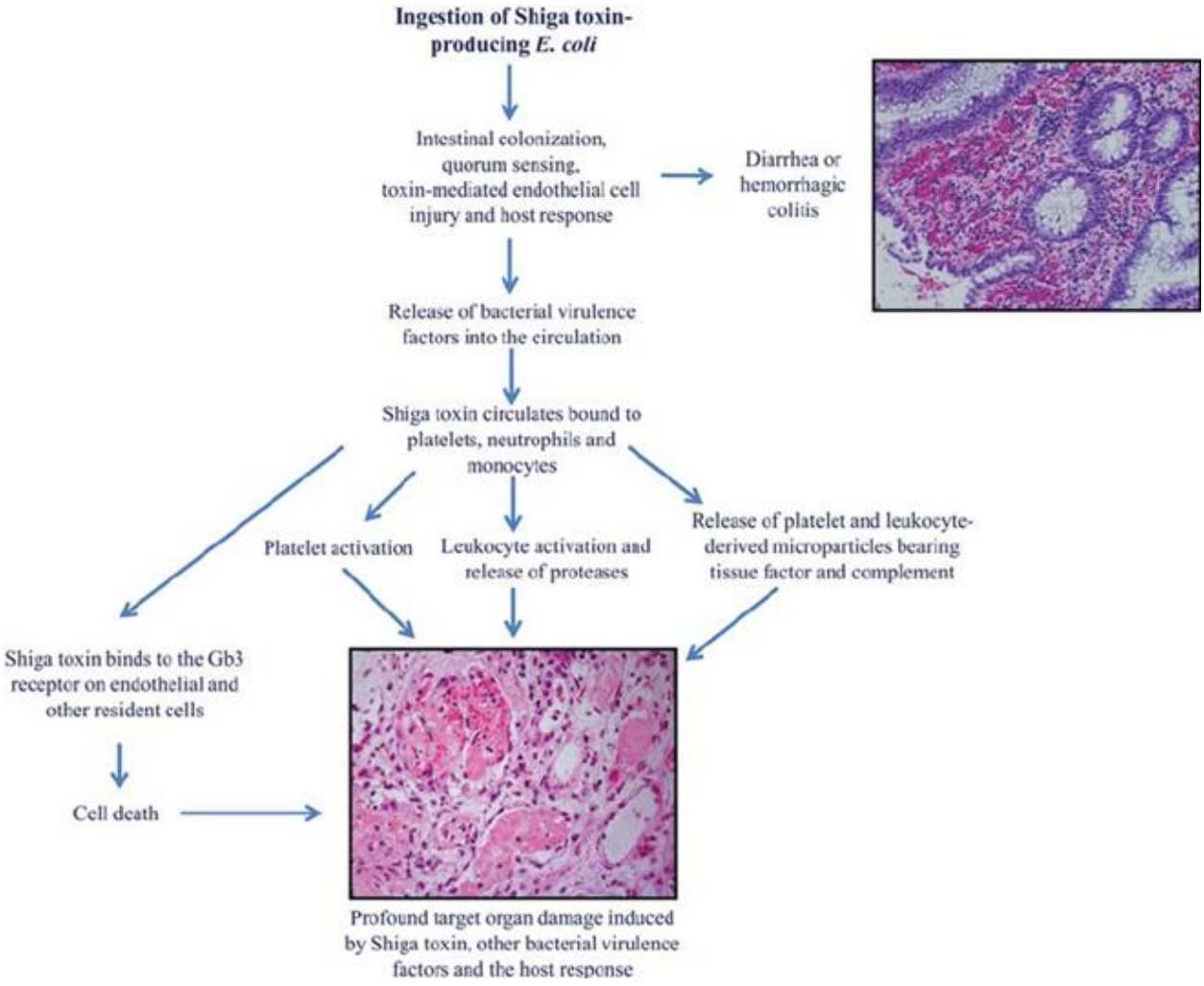

Figure 2.12: Pathogenesis of *STEC* (Karpman, 2012)

2.7 Biofilm and diseases:

Compared to their planktonic counterparts, biofilm producing microorganisms have different characteristics like resistance to host defenses, antibiotics treatment and unique growth rates. This resistance to host defenses is caused by the production of antibodies that cannot penetrate the biofilm surface. Besides, although antimicrobial treatment might initially have an effect, after completion of the antibiotic therapy frequent relapses occur as bacteria inside the biofilm remain unaffected due to incomplete antimicrobial penetration. In addition, within a biofilm bacteria can transfer extrachromosomal genetic elements- resistance plasmids, further causing resistance in bacteria. Biofilm-related infections are frequently caused by *Staphylococcus epidermidis*,

Gardnerella vaginalis, Candida albicans, Pseudomonas aeruginosa, Klebsiella pneumoniae and *Enterococcus faecalis* etc (Del Pozo, 2018).

2.8 Cholera Biofilm and epidemics:

In March 2022, a cholera outbreak striked Dhaka city as around 1200 cholera patients from different areas were admitted in the hospitals, mainly the ones run by the International Centre for Diarrhoeal Disease Research, Bangladesh (icddr,b). This year, the number of patients was higher than normal, as the hospital authority claimed each day nearly a thousand of patients visited complaining about diarrhea and cholera ("Dhaka Wasa must answer for cholera outbreak", 2022).

The two *V. cholerae* serotypes O1 and O139 are responsible for cholera epidemics and pandemics, causing a significant health issue in many countries in Asia, Africa, and Latin America (Alam et al., 2007). In Bangladesh, cholera outbreaks are observed from March to May, followed by a second outbreak from September to October, suggesting the seasonal cycle of *V. cholerae* (Faruque et al., 2005). During cholera epidemics, the presence of biofilm fragments containing aggregates of *V. cholerae* was isolated from cholera stool. Although these cells were initially found to be infective and culturable, they soon lost their infectivity, indicating a temporal constraint. Thus, these cells can only intensify the cholera epidemics in areas with poor sewage treatment facilities (Alam et al., 2007). Therefore, the question remains: what contributes to the annual seasonal outbreaks of cholera?

Throughout the year in Bangladesh, *V. cholerae* O1 remains in the aquatic environment as nonculturable coccoid cells in biofilms that can be detected using fluorescent antibody-based studies. The cells derived from these biofilms could be made culturable even after a year of dormancy, accounting for the annual cycle and epidemics of cholera. The resuscitation of *V. cholerae* in nature is usually expected to be caused by the fluctuations in temperature, nutrient levels, and the zooplankton (host of *V. cholerae*) blooms during summer. Surprisingly, the resuscitation was only observed when the cells were bound in biofilms, not in nonculturable microcosms (Alam et al., 2007). During epidemics, water samples showed the presence of single cells and biofilm-bound *V. cholerae* O1 in culturable state, however the rest of the year, these cells remained in a nonculturable state as a reservoir for the recurrent annual epidemics (Sultana et al., 2018).

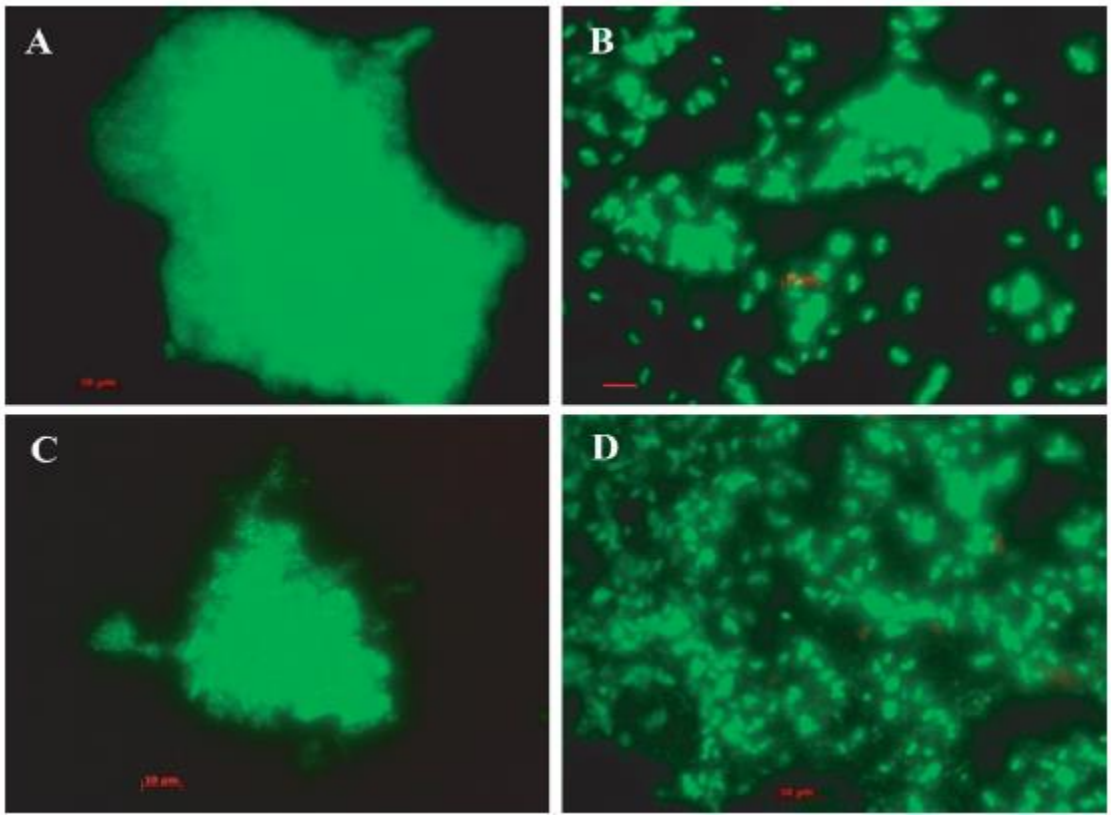

Figure 2.13: Direct fluorescent monoclonal antibody (DFA) detection of *V. cholerae* O1 in aquatic ecosystem of the Bay of Bengal shows biofilms of *V. cholerae* O1 during winter and monsoon months- A and C, and free-living *V. cholerae* O1 cells during spring and fall months- B and D (Sultana et al., 2018)

2.9 ELISA

In this experiment, the optical density (OD) was measured using an Enzyme Linked Immunosorbent Assay (ELISA). Micro ELISA autoreader technique is an effective way of measuring the OD of a biofilm (Mosharraf et al., 2020).

ELISA is a widely used procedure in almost every immunology lab. It depends on the principle of antigen- antibody interaction. This interaction can then be quantified using ELISA Auto reader machines by measuring the OD. Substances like peptides, proteins, antibodies, and hormones can be identified and measured using ELISA. ELISA has many other names and derivations like EIA, RIA, ELISPOT (Lequin, 2005) etc. However there are three main types of ELISA. Those are:

- Direct ELISA
- Indirect ELISA
- Sandwich ELISA

In this experiment none of these techniques were used. Only the OD measuring property of ELISA Auto reader was used to get the OD of the biofilms formed inside ELISA plates.

2.10 Coomassie Stain and Dissolving Coomassie Stain with Glacial Acetic Acid

Coomassie Brilliant Blue G-250 is a disulfonated triphenylmethane dye. They are mainly used to dye proteins as they attach to protonated basic amino acids like lysine, arginine, and histidine through electrostatic contact and hydrophobic interactions with aromatic residues. As the CBB G-250 dye is non-covalent and reversible, they do not interfere with the mass spectrophotometry of the dyed biofilm rings (Steinberg, 2009). The biofilms in question are dyed by the CBB G-250 on the basis of the extracellular proteins secreted by the bacteria encased inside the biofilm, the extracellular matrix proteins present in VPS, the adhesins, pili and flagella which are components of a typical biofilm structure. Three of the major proteins present in the VPS are RbmA, Bap1, and RbmC which are important for biofilm formation along with extracellular chitin-binding protein GbpA which are used for the mediation of attachment of the biofilm structure to a chitinous surfaces of a zooplankton (Fong, 2015). As a result, these proteins are the target components of the biofilm used by the CBB G-250 for dyeing and visualization in the study. Proteins bind to CBB G-250 in an acidic condition, and their positive charges prevent protonation, resulting in a blue color. The dye's absorption maximum shifts from 465 to 595 nm when it binds to a protein, and it is the rise in absorbance at 595 nm that is measured in Phase 2 of the study that will be discussed in detail later in the paper (Roger, 2017).

Coomassie stains bound to the biofilm can be solubilized using 33% glacial acetic acid (Stepanović et al., 2000).

Chapter 3:

Materials

And

Methods

3. Materials and Methods:

3.1 Organisms:

To conduct this study, 4 strains of bacteria were used. These include:

1. *Shiga toxin-producing Escherichia coli (STEC)*
2. *Vibrio Cholerae 1877* (HapR mutated)
3. *Vibrio Cholerae 1712* (LuxO induced)
4. *Vibrio Cholerae WT324*

3.2.1 Bacterial Culture Media:

Luria Broth (LB) and LB Agar media were used in this experiment. All the organisms here are gram negative bacteria and LB is well suited for their growth. Other than that 0.8% LB Agar media was used as preservation media. Bacterial stocks were kept in that and covered by paraffin oil.

All the cultures and media were taken from Life Science Laboratories, BRAC University. They were revived, used and maintained using standard protocols.

3.2.2 Biochemical Tests

A number of biochemical tests were done to confirm the bacterial strains used in this experiment. In order to confirm whether the vibrio cholera strains were actually vibrio, they were tested using Thiosulfate-citrate-bile salts-sucrose (TCBS) agar media. After streak plating the *Vibrio cholerae* strains on the TCBS agar media plate and incubating it at 37°C for 24 hours, if the green TCBS agar turned yellow then the strains were confirmed to be vibrio cholerae and if they remained green or any other colour they were said to be otherwise. After TCBS plating, all three *V.cholerae* strains gave yellow colonies while STEC remained green.

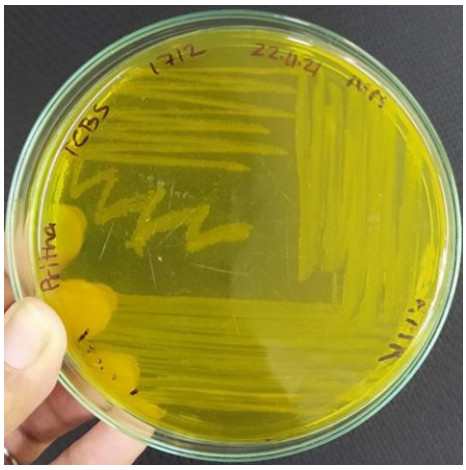

Figure 3.1: *1712 V.cholerae* showing yellow colonies in TCBS agar plate

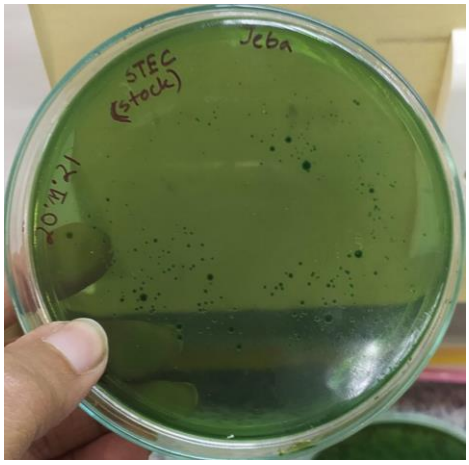

Figure 3.2: *STEC* showing green colonies in in TCBS agar plate

In order to confirm the *STEC* as *E.coli*, it was tested on triple sugar iron agar (TSI). An inoculation needle was used to pick up *STEC* colonies from an LA plate containing *STEC* and a needle was used to stab the TSI slant agar and while bringing out the needle, the slant surface of the agar media was streaked using the same needle. The inoculated TSI test-tubes were then incubated at 37°C for 24 hours. The test-tubes that gave a yellow slant and butt were confirmed to be *STEC*.

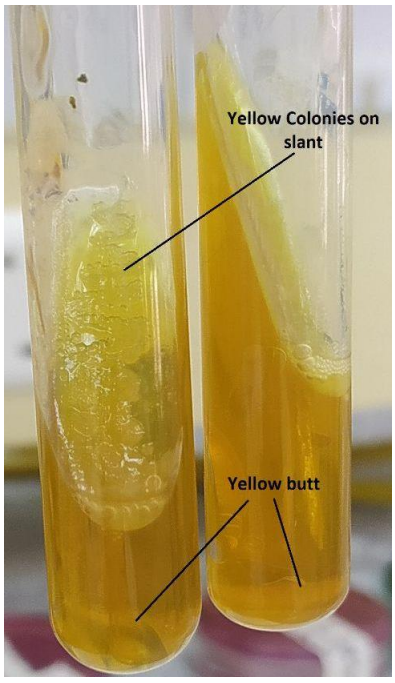

Figure 3.3: *STEC* showing yellow colonies on slant and a yellow butt on TSI media

The *STEC* also gave yellow colonies in XLD agar media plates when streaked and incubated at 37°C for 24 hours which confirmed it as an *E.coli* strain. These tests were done periodically in order to maintain the proper bacterial strains throughout the study.

3.3 Overview of the Methods:

At first, the strains were revived from the bacterial stocks, and fresh cultures were prepared. These fresh cultures were inoculated in fresh LB and left in the shaker incubator overnight. From this active cultures were prepared which were placed in vials/falcon tubes/ ELISA plates to form static biofilms.

After biofilms are formed, they are divided into two sets where one was exposed to the sunlight and the other was kept in the dark for the same time. The characteristics of the biofilms were then determined by 4 different phases. In these phases, the cell count in the biofilms, the OD of the biofilms and OD of the stained biofilms were measured. In addition, the changes in the thickness of the biofilm over the period was also observed by staining and imaging.

3.4 Revival of Bacterial Culture:

The bacterial strains were revived from the laboratory stocks preserved in T1N1 media. Using streak plate method, the cultures from the stocks were revived by making subculture on LB agar plates. These were incubated for 24 hours in a 37℃ incubator, and single colonies were isolated from these plates.

3.5 Making Young Culture and Biofilm:

To prepare young culture, single colonies from the agar plates were taken to inoculate 1 ml LB in eppendorf tubes. This was left overnight in a shaker incubator to produce the overnight culture. 500 µL of this overnight culture were then added to 9.5ml fresh LB in test tubes/falcon tubes and was left in the shaker incubator until turbidity was observed. These young cultures were then transferred to the glass vials, falcon tubes, and ELISA plates and left uninterrupted for 72-96 hours to ensure biofilm formation. For phase 3, a coverslip was inserted into the falcon containing the young culture so that the coverslip was only half submerged.

3.6 Discarding Old Culture and Adding New Media

After 72 hours of biofilm formation, the old cultures were discarded and new media was added. From the vials, at first, the biofilm layer formed on the top of the culture was carefully removed using micropipette tips. Then, the old culture was gently removed using a micropipette ensuring the biofilm ring on the vial surface remained untouched. The vial/falcon tubes were washed two times with sterilized LB media to ensure removal of most of the bacteria and surface biofilm. Finally, fresh LB was added to the vials, usually 1000 µL, enough to completely submerge the biofilm rings in vials and 20ml in falcon tubes to fully submerge the coverslips containing the biofilm.

After 96 hours of biofilm formation, the coverslips were removed from the old cultures in the falcon tubes, separated, gently rinsed with sterile saline and inserted into the falcon tubes containing the fresh LB media. It was rinsed with saline to remove the extra layer of biofilm from the cover slip. The coverslips were fully submerged in the media.

3.7 Exposure in Sunlight and Darkness

Phases

3.7.1 Phase 1: Glass vials

In this phase, the 72-hour biofilms made in the glass vials were divided into 2 sets and then exposed to sunlight and darkness for 6 hours periodically. Each set contained 4 vials of each of the 4 bacterial strains. On the first day, one of the vials from the 2 sets were separated from the set to collect the data in 0 hours of sunlight and darkness. For 3 consecutive days, the vials were kept in the sunlight and dark for 6 hours, and after 6 hours each day, the cultures were plated using droplet method, and the vials were stained to visually observe the changes in the biofilm rings.

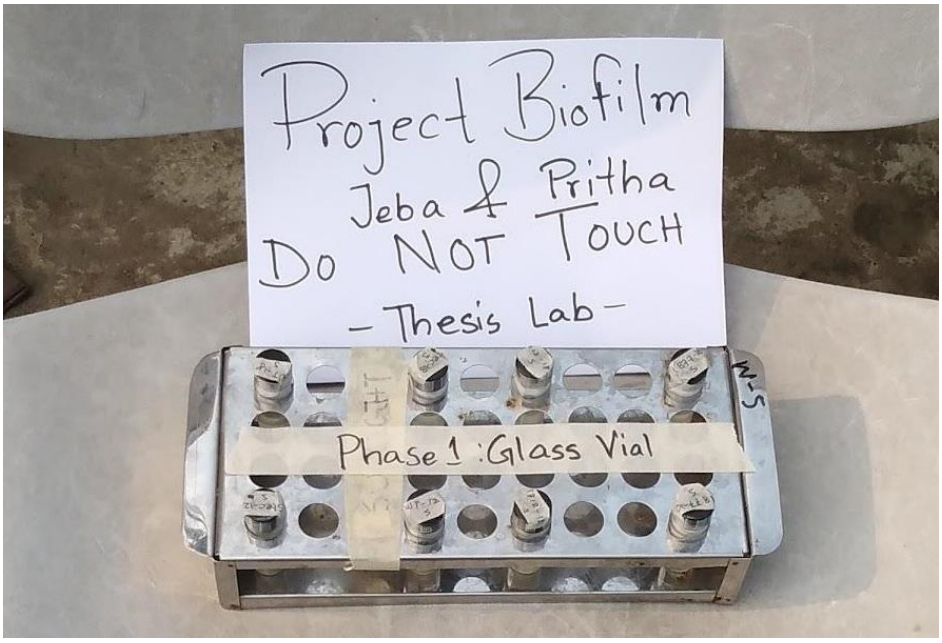

Figure 3.4: Exposure of glass vials containing bacterial biofilm to sunlight as part of phase 1 data collection.

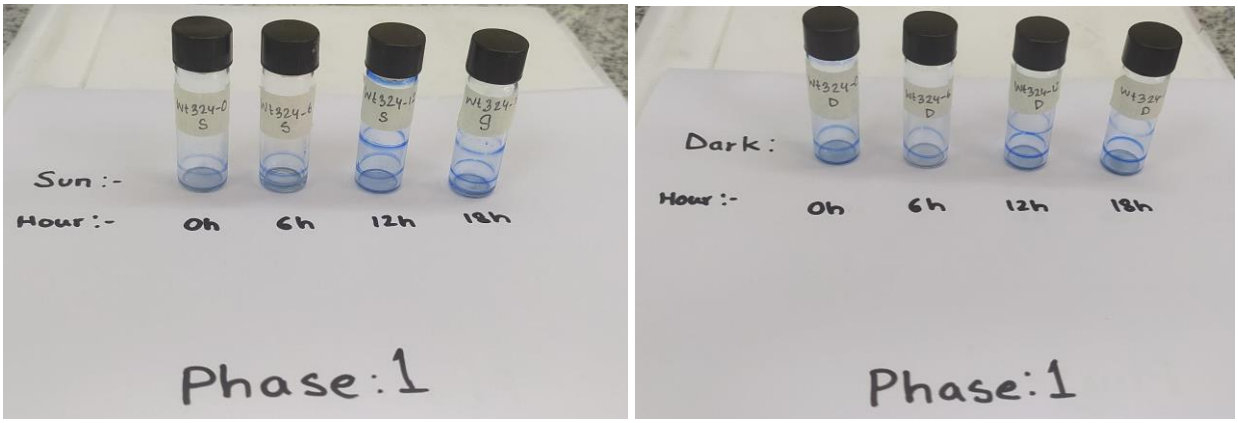

Figure 3.5: The changes in the biofilm ring of *Vibrio WT324* strain due to exposure of sunlight and darkness over a period of 18 hours. The blue rings inside the glass vials are biofilm rings that were stained with CBB G-250 solution overnight and then washed with saline

3.7.2 Phase 2: Optical Density of Dissolved Biofilm Rings

In this phase, the biofilm rings that were stained using CBB G250 were dissolved using 33% glacial acetic acid. Using a micropipette, enough glacial acetic acid was poured into the vials in order to submerge the lower biofilm rings so that the stain gets dissolved into the solution. For the vials where a second biofilm was formed after exposure, glacial acetic acid was carefully poured in order to avoid making contact with the upper ring and only dissolve the lower biofilm ring. After slightly shaking the vials, the stain gets dissolved into the solution giving a blue solution. 200µL of this solution was then transferred into the appropriately labeled wells of a non-autoclavable 96 well ELISA plate and the OD was then measured using a MultiscanEX ELISA Machine at 450nm absorbance.

Figure 3.6: CBB G-250 stained biofilm ring dissolved by 33% glacial acetic acid forming a blue solution of different blue color spectrum according to the thickness of the biofilm rings used for phase 2 data collection

3.7.3 Phase 3: Coverslips

In this phase, 96-hour biofilms formed on the coverslips were inserted into the falcon tubes. These falcon tubes were also divided into 2 sets, where set 1 was exposed to the sunlight for 6 hours and set 2 was kept in the dark for 2 consecutive days. Each set contained 6 falcon tubes, and 2 were separated from each set before exposing them to sunlight or darkness respectively to obtain 0 hour data. After 6 hours of exposure, each day, plating and staining was done to observe the changes in the biofilm structure and the presence of any planktonic bacteria in the LB media.

Figure 3.7: Exposure of coverslips containing bacterial biofilm inside falcon tubes containing LB media to sunlight as part of phase 3 data collection.

a. b.

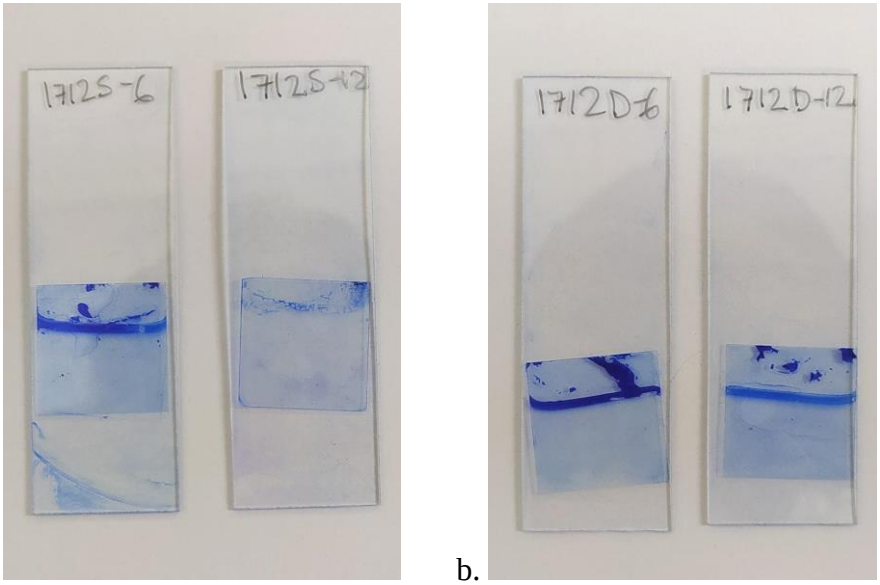

Figure 3.8: The changes observed in the biofilm layers on the coverslips of *1712 Vibrio* strain due to the exposure of sunlight and darkness over a period of 12 hours. a) shows the effect of sunlight on the biofilm while b) shows the effect of darkness on the biofilm.

3.7.4 Phase 4: OD of biofilm formed in ELISA plates

In phase 4, biofilm was formed on two sterile ELISA plates for 72 hours. One of the plates were exposed to the sunlight for 6 hours, and the other was kept in the dark. This was repeated for 3 days. The OD was measured using MultiscanEX ELISA Machine after every 2 hours. Each plate contained multiple replicates of the same biofilm to derive an average value of the OD to reduce errors (Mosharraf et al., 2020).

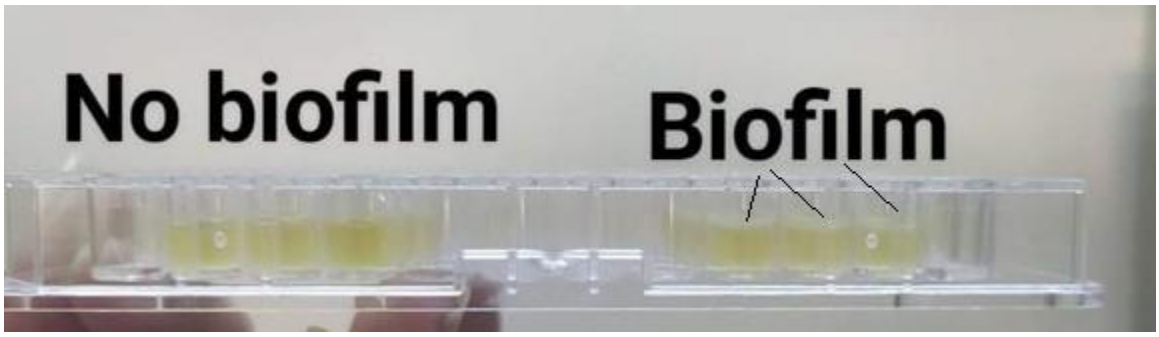

Figure 3.9: **Active culture media in 96 well ELISA plate for biofilm formation.** In this image, it is visible that the wells on the right have clear white biofilm layers on the surface of the LB media whereas the wells on the left have no biofilm layers.

3.8 Plating the Exposed Biofilm Cultures

At first, using a micropipette tip, the unattached biofilm layer was removed from the top. About 100 µL culture was collected from the glass vials and falcon tubes, and serial dilution was carried out. For serial dilution, 100 µL culture was added then, using the drop plate method, plating was done for about 4 dilutions of each strain. For every dilution, 3 drops of cultures were added for every quadrant. The cell count obtained in this method helped to identify the number of bacteria coming out of the biofilm. Comparing the count over the hours of both sunlight and dark helped to determine the effects of sunlight exposure on the bacterial biofilms.

Before plating, antibiotics were spread on the petri dishes using the spread plate method. The use of antibiotics ensured the growth of the desired bacterial strains only. The antibiotics used and the volumes for each respective strains are given below:

Bacterial strain	Antibiotic used	Working Concentrations	Volume of antibiotic used
V. cholerae 1877	Kanamycin	10mg/ml	100 µL
V. cholerae 1712	Metronidazole	0.02mg/ml	80 µL
V. cholerae WT324	Metronidazole	0.02mg/ml	80 µL
STEC	Vancomycin	1mg/ml	100 µL

Table 1: The table shows the name of the antibiotic and the amount used for the respective bacterial strains.

3.9 Biofilm Staining and Washing

The vials and the coverslips were gently washed with sterile saline (0.9N NaCl), dried, and stained with Coomassie Brilliant Blue G-250 dye. The dye was left overnight to completely stain the biofilm, and then was washed with sterile saline to remove excess dye.

Figure 3.10: Coomassie Blue dye prepared to stain the biofilms using CBB G-250 powder

3.10 Dissolving Stained Biofilm Rings

In phase 2, the stained biofilm rings were first rinsed with sterile saline to remove excess dye. Then, glacial acetic acid was added to the rings, which immediately dissolved the stains. The vials containing biofilm rings stained a week were dissolved and transferred to 96-well ELISA plates to measure the OD of the biofilm rings. The OD obtained showed clear changes in the biofilm occurring due to exposure in sunlight and darkness.

A second biofilm ring formed in the glass vials after 6-12 hours. It was made sure to only dissolve the first biofilm ring, not the second one, to obtain the desired results.

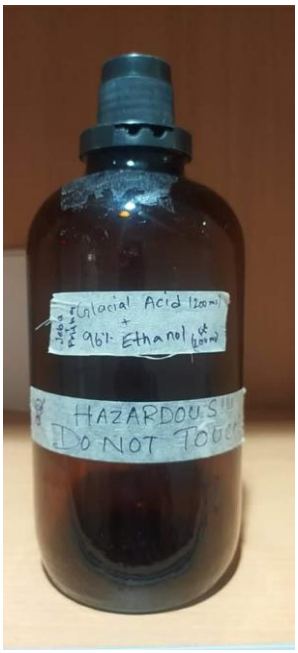

Figure 3.11: 33% glacial acetic acid used to dissolve stained biofilm rings

3.11 ELISA of Biofilm Stains

The stains on the biofilm rings formed in the vials were dissolved using glacial acetic acid. 200 µL of the dissolved stain were then transferred into the 96-well ELISA plate. The reading was measured using MultiscanEX ELISA Machine. For every 6 hours, a replicate was kept to calculate the average OD.

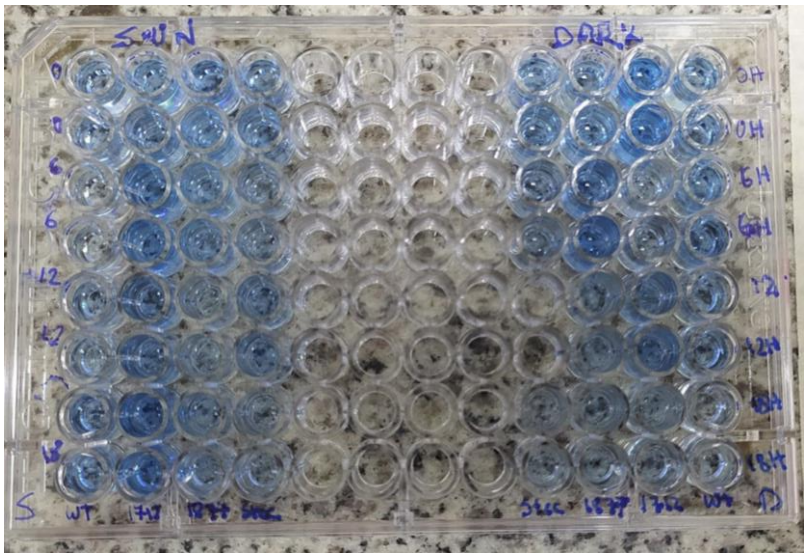

Figure 3.12: **Dissolved biofilm stains in 96 well ELISA plate**. In phase 2, using glacial acetic acid, the stained biofilm rings were dissolved and 200 µL of the dissolved stain solution was used to fill each well of the ELISA plates. Two replicates were kept for every 6 hours.

3.12 ELISA of Biofilms

MultiscanEX ELISA Machine by Thermo Scientific was used to measure the absorbance of the biofilms, at 450 nm wavelength. Each day, readings were recorded after every 2 hours interval. Some of the wells were filled with media as a negative control.

Figure 3.13: MultiscanEX ELISA Machine by Thermo Scientific

3.13 Statistical analyses

Statistical analysis was performed using Microsoft Excel and StataMP-64 analytical software version 16 for Windows. The statistical differences between two groups was assessed by independent samples T Test assuming equal variances. The level of significance was considered to be 0.05. In this study, two-tailed t Tests were performed.

Chapter 4:

Results

4.1.1 PHASE 1: Biofilms formed on Glass Vials

a. 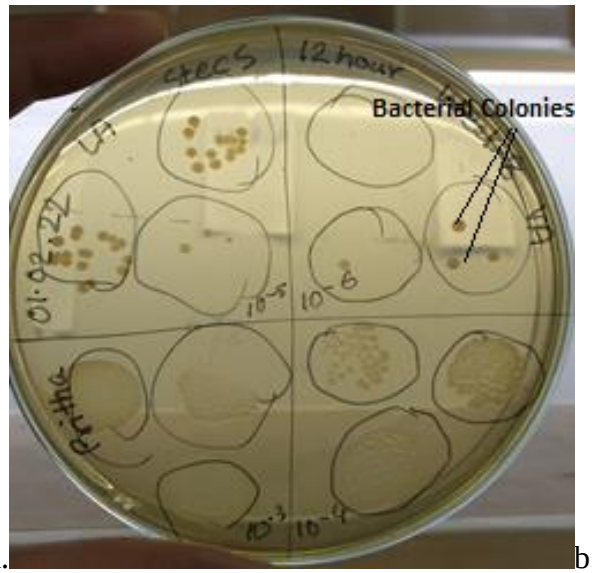

b. 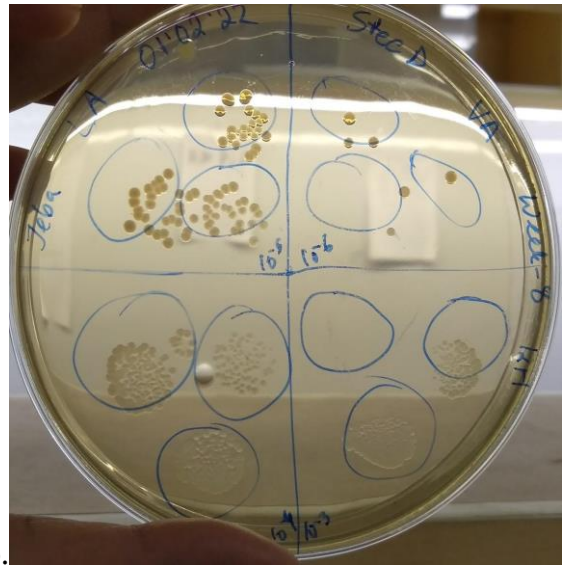

c. 
d. 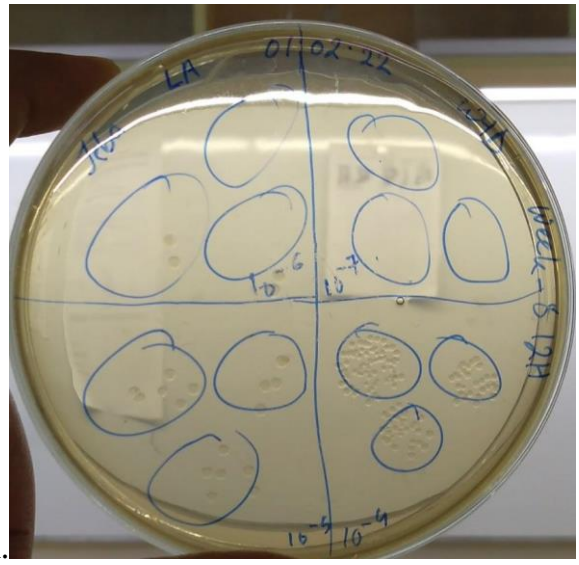

e. 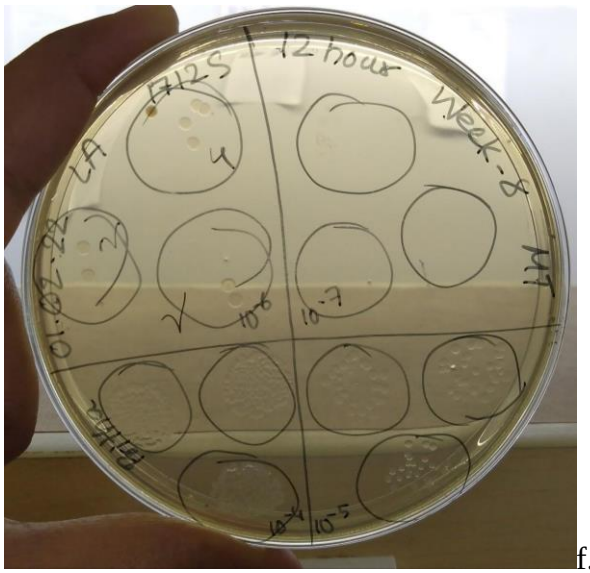 f. 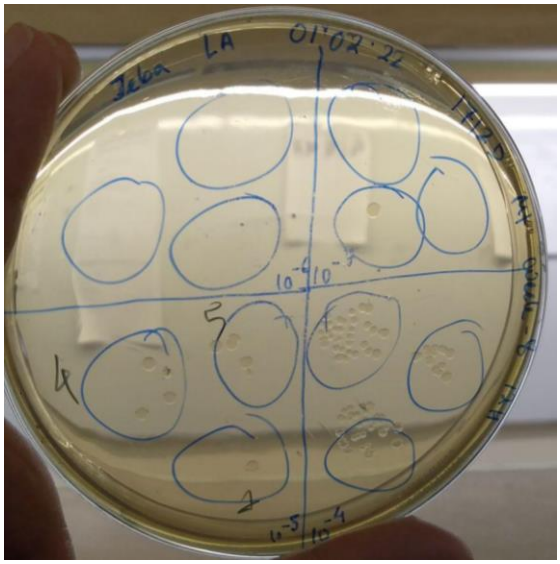

Figure 4.1**: Petri dishes showing the colonies of the respective bacterial strains**. The plates contain 24 hour bacterial colonies plated using the droplet method and containing the dilution factors of 10^4, 10^5, 10^6 and 10^7. a) contains colonies from culture of *STEC* after the biofilm was exposed to 12 hours of sunlight, b) contains colonies from culture of *STEC* after the biofilm was exposed to 12 hours of darkness, c)contains colonies from culture of *1877 Vibrio* after the biofilm was exposed to 12 hours of darkness, d) contains colonies from culture of *WT324 Vibrio* after its biofilm was exposed to 12 hours of darkness, e) contains colonies from culture of *1712 Vibrio* after the biofilm was exposed to 12 hours of sunlight, f) contains colonies from culture of *1712 Vibrio* after the biofilm was exposed to 12 hours of darkness. The dots are bacterial colonies.

4.1.2 Phase 1 Graphs and Regression Analysis

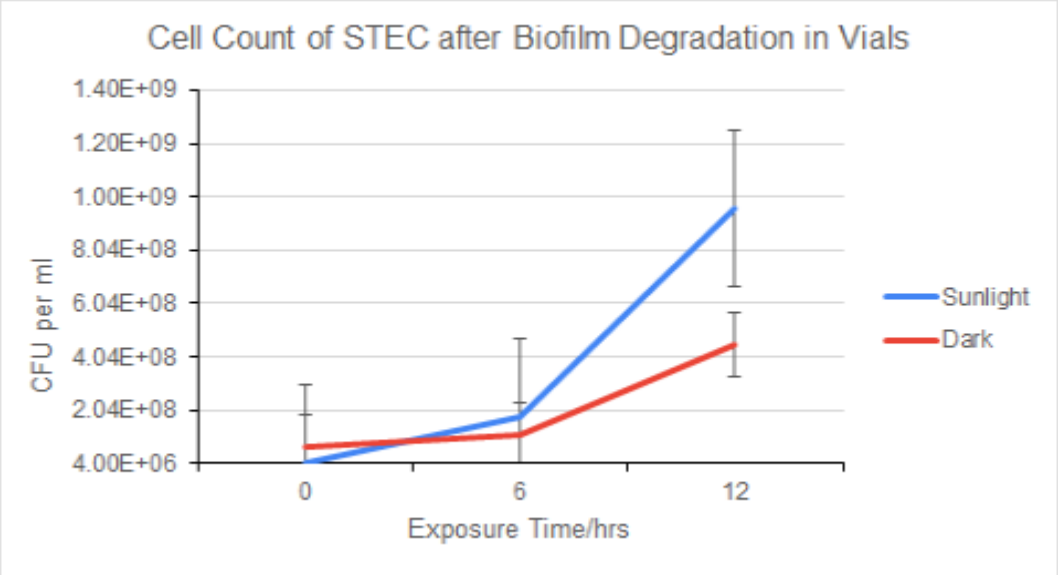

Figure 4.2: Graphical representation of cell count of *STEC* after biofilm degradation in sunlight and in darkness taken from phase 1 data. X axis represents the exposure time in hours and Y axis represents CFU per ml

Organism	r value and interpretation	R2 value and interpretation	Regression model and interpretation
STEC SUNLIGHT	0.9379 Strong Positive Correlation	R2 = 0.8797 87.97% of the total variation of the cell count can be explained by the regression model.	y = -9.77E+07 + 7.95E+07x When time of exposure in sunlight is 0 hour, cell count will be 9.77E+07 CFU/ml. And when time of exposure will increase by 1 hour, cell count will increase by 7.95E+07 CFU/ml.
STEC DARK	0.9168 Strong Positive Correlation	R2 = 0.8406 84.06% of the total variation of the cell count can be explained by the regression model	y = 2.03E+07 + 3.17e+07x When time of exposure in the dark is 0 hour, cell count will be 2.03E+07 CFU/ml. And when time of exposure will increase by 1 hour, cell count will increase by 3.17e+07 CFU/ml.

Table 2: R value, R square value, regression model and their respective interpretations for *STEC* exposed to winter sunlight and darkness taken from phase 1 data

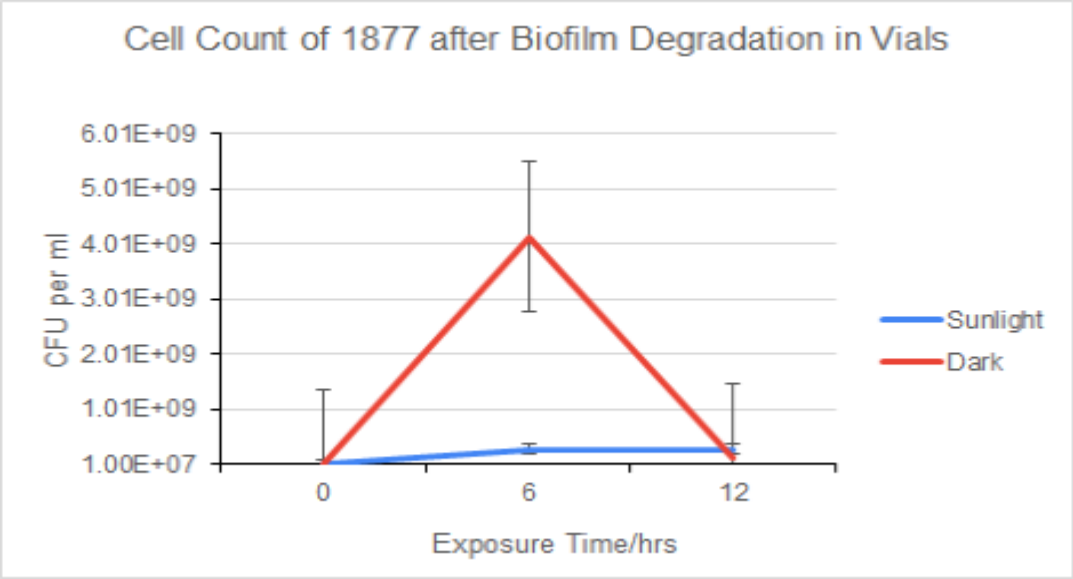

Figure 4.3: Graphical representation of cell count of *Vibrio 1877* after biofilm degradation in sunlight and in darkness taken from phase 1 data. X axis represents the exposure time in hours and Y axis represents CFU per ml

Organism	r value and interpretation	R2 value and interpretation	Regression model and interpretation
1877 SUNLIGHT	0.8662 Strong Positive Correlation	R2 = 0.7503 75.03% of the total variation of the cell count can be explained by the regression model.	y = 5.73e+07 + 2.20e+07x When time of exposure in sunlight is 0 hour, cell count will be 5.73e+07 CFU/ml. And when time of exposure will increase by 1 hour, cell count will increase by 2.20e+07 CFU/ml.
1877 DARK	0.9403 Strong Positive Correlation	R2 = 0.0005 0.05% of the total variation of the cell count can be explained by the regression model	y = 1.38e+09 + 8.37E+06x When time of exposure in the dark is 0 hour, cell count will be 1.38e+09 CFU/ml. And when time of exposure will increase by 1 hour, cell count will increase by 8.37E+06 CFU/ml.

Table 3: R value, R square value, regression model and their respective interpretations for *Vibrio 1877* exposed to winter sunlight and darkness taken from phase 1 data

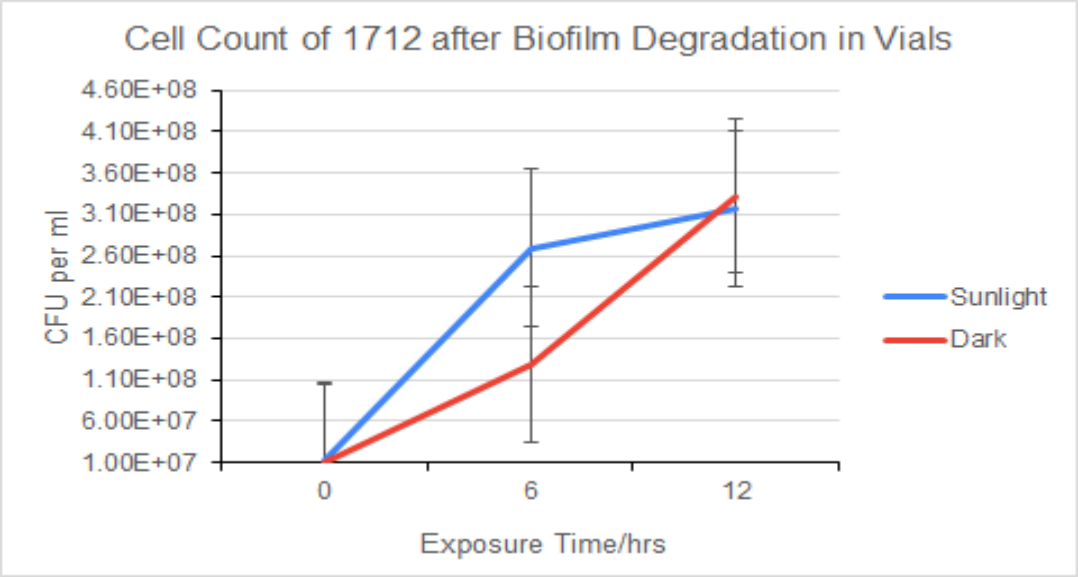

Figure 4.4: Graphical representation of cell count of *Vibrio 1712* after biofilm degradation in sunlight and in darkness taken from phase 1 data. X axis represents the exposure time in hours and Y axis represents CFU per ml

Organism	r value and interpretation	R2 value and interpretation	Regression model and interpretation
1712 SUNLIGHT	0.9293 Strong Positive Correlation	R2 = 0.8635 86.35% of the total variation of the cell count can be explained by the regression model.	y = 4.73e+07 + 2.54e+07x When time of exposure in sunlight is 0 hour, cell count will be 4.73 e+07 CFU/ml. And when time of exposure will increase by 1 hour, cell count will increase by 2.54e+07 CFU/ml.
1712 DARK	0.9882 Strong Positive Correlation	R2 = 0.9765 97.65% of the total variation of the cell count can be explained by the regression model	y = -3.54E+06 + 2.68e+07x When time of exposure in the dark is 0 hour, cell count will be 3.54E+06 CFU/ml. And when time of exposure will increase by 1 hour, cell count will increase by 2.68e+07 CFU/ml.

Table 4: R value, R square value, regression model and their respective interpretations for *Vibrio 1712* exposed to winter sunlight and darkness taken from phase 1 data

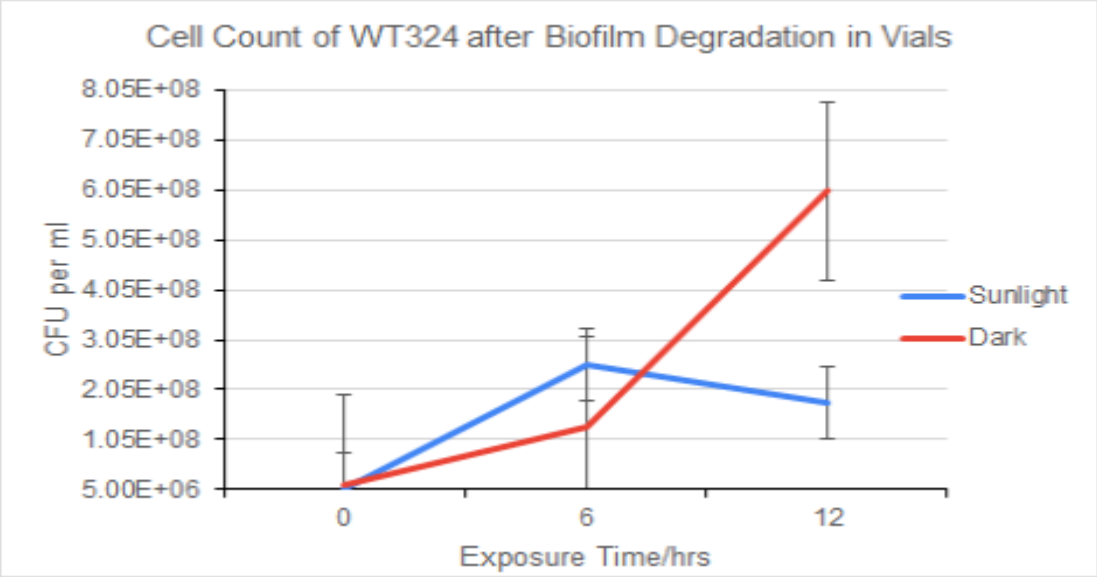

Figure 4.5: Graphical representation of cell count of *Vibrio WT324* after biofilm degradation in sunlight and in darkness taken from phase 1 data. X axis represents the exposure time in hours and Y axis represents CFU per ml

Organism	r value and interpretation	R2 value and interpretation	Regression model and interpretation
WT324 SUNLIGHT	0.6787 Moderate Positive Correlation	R2 0.4607 46.07% of the total variation of the cell count can be explained by the regression model.	y = 5.94e+07 + 1.45e+07x When time of exposure in sunlight is 0 hour, cell count will be 5.94e+07 CFU/ml. And when time of exposure will increase by 1 hour, cell count will increase by 1.45e+07 CFU/ml.
WT324 DARK	0.9403 Strong Positive Correlation	R2 = 0.8892 88.92% of the total variation of the cell count can be explained by the regression model	y = -4.39e+07 + 4.89e+07x When time of exposure in the dark is 0 hour, cell count will be 4.39e+07 CFU/ml. And when time of exposure will increase by 1 hour, cell count will increase by 4.89e+07 CFU/ml.

Table 5: R value, R square value, regression model and their respective interpretations for *Vibrio WT324* exposed to winter sunlight and darkness taken from phase 1 data

4.1.3 T-TEST RESULTS FOR BIOFILMS FORMED ON VIALS:

Null Hypothesis: There is no significant difference between cell count in winter sun and winter dark

Alternative Hypothesis: There is a significant difference between cell count in winter sun and winter dark

ORGANISM	Time/hour	p-value	Interpretation	NULL HYPOTHESIS	Overall remarks
STEC SUN VS. STEC DARK	0	0.37	0.37 > 0.05	ACCEPT	NULL HYPOTHESIS IS ACCEPTED
	6	0.65	0.65 > 0.05	ACCEPT	
	12	0.57	0.57 > 0.05	ACCEPT	
1877 SUN VS. 1877 DARK	0	0.64	0.64 > 0.05	ACCEPT	NULL HYPOTHESIS IS ACCEPTED
	6	0.38	0.38 > 0.05	ACCEPT	
	12	0.51	0.51 > 0.05	ACCEPT	
1712 SUN VS. 1712 DARK	0	0.90	0.90 > 0.05	ACCEPT	NULL HYPOTHESIS IS ACCEPTED
	6	0.28	0.28 > 0.05	ACCEPT	
	12	0.92	0.32 > 0.05	ACCEPT	
WT324 SUN VS. WT324 DARK	0	0.46	0.46 > 0.05	ACCEPT	NULL HYPOTHESIS IS ACCEPTED
	6	0.61	0.61 > 0.05	ACCEPT	
	12	0.23	0.23 > 0.05	ACCEPT	

Table 6: Statistical significance comparison between the cell counts taken from phase 1 data of biofilms exposed to winter sunlight and winter darkness by T-test

4.1.4 Interpretation of the Statistical Analysis of Phase 1 Data

According to the graphical representations, the cell count increases with time in both sunlight exposure and the dataset that was kept in the dark *(Fig. 4.2, Fig.4.3, Fig.4.4)*, with the exception of *Vibrio WT324*, where the cell count decreased in the second 6 hours for the data set that was exposed to sunlight *(Fig.4.5)*. This increase is corroborated by the r value which shows moderate to strong positive correlation between cell count and the exposure time. The regression models give quantitative values of the cell count increase with each hour increase in exposure time. These values are: 7.95E+07 CFU/ml and 3.17E+07 CFU/ml in sunlight and darkness respectively for

STEC, 2.20E+07 CFU/ml and 8.37E+06 CFU/ml in sunlight and darkness respectively for *Vibrio 1877*, 2.54E+07 CFU/ml and 2.68E+07 CFU/ml in sunlight and darkness respectively for *Vibrio 1712*, 1.45E+07 CFU/ml and 4.89E+07 CFU/ml in sunlight and darkness respectively for *Vibrio WT324 (Table 2-5)*. However, even though the graphical representation and the regression model shows that the cell count increases in the data set that was exposed to sunlight, a t-test was done to show the level of significance for this increase. According to the t-tests, there is no significant difference between the cell count of the biofilms exposed to sunlight and the ones kept in darkness during the winter season *(Table 6)*. This conclusively shows that the sunlight does not significantly break the bacterial biofilms to resuscitate a significant amount of planktonic bacteria during the winter season.

4.2.1 PHASE 2: OD of Biofilm Rings Stained with Coomassie Blue Dye

Average OD of stained biofilm exposed to sunlight:

Time/ Bacterial strains	*STEC*	*V. cholerae WT324*	*V. cholerae 1712*	*V. cholerae 1877*
0 hours	0.05525	0.0575	0.063	0.06325
6 hours	0.059	0.056	0.06275	0.0665
12 hours	0.061	0.073	0.06875	0.073
18hours	0.06875	0.0645	0.08	0.07925

Table 7: Average OD of stained biofilm exposed to sunlight, obtained using ELISA at 450 nm

Average OD of stained biofilm exposed to darkness:

Time/ Bacterial strains	*STEC*	*V. cholerae WT324*	*V. cholerae 1712*	*V. cholerae 1877*
0 hours	0.056	0.0645	0.0655	0.061
6 hours	0.0565	0.07375	0.0615	0.072
12 hours	0.04325	0.0795	0.07925	0.0775
18hours	0.05825	0.06925	0.07325	0.06625

Table 8: Average OD of stained biofilm exposed to darkness, obtained using ELISA at 450 nm

4.2.2 Phase 2 Graphs and Regression Analysis

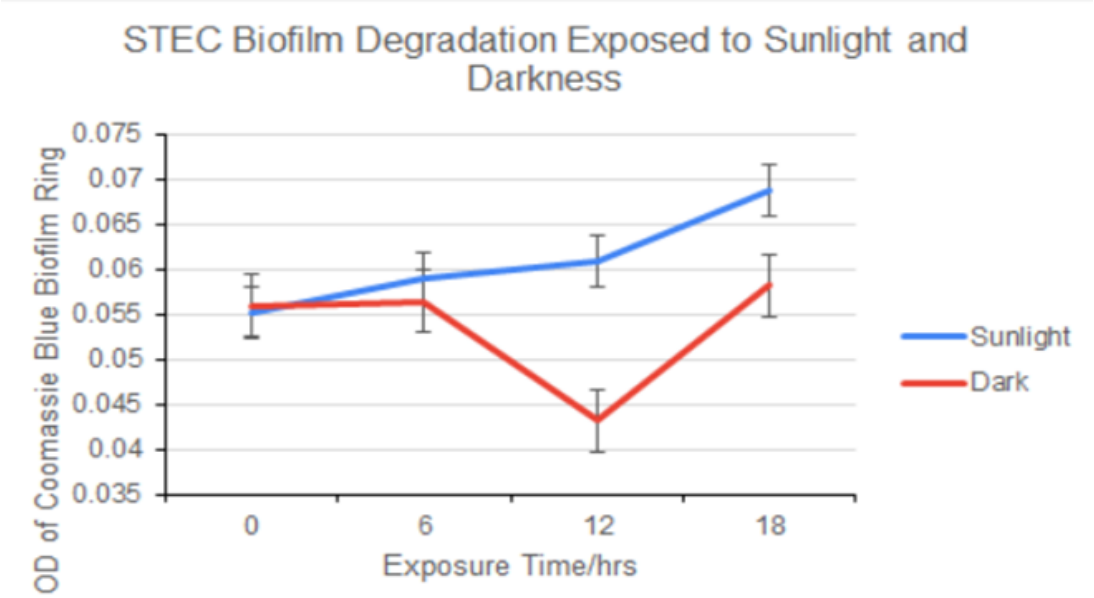

Figure 4.6: Graphical representation of OD of CBB G-250 stained biofilm rings of *STEC* after biofilm degradation in sunlight and in darkness taken from phase 2 data. X axis represents the exposure time in hours and Y axis represents OD of coomassie blue stained biofilm rings

Organism	R value and interpretation	R2 value and interpretation	Regression model and interpretation
STEC SUNLIGHT	0.9643 Strong Positive Correlation	R2 = 0.9299 92.99% of the total variation of OD of biofilm stain OD can be explained by the regression model.	y = 0.054625 + 0.0007083x When time of exposure is 0 hour, the OD of biofilm stain will be 0.054625. And when time of exposure increases by 1 hour, OD of biofilm stains will increase by 0.0007083.
STEC DARK	-0.1216 Weak negative correlation	R2 = 0.0148 The R-squared value is 0.9299, so 92.99% of the total variation of OD of biofilm stain OD can be explained by the regression model.	y = 0.054475 - 0.0001083x When the time of exposure is 0 hour, the OD of biofilm stain will be 0.054475. And when time of exposure increases by 1 hour, OD of biofilm stains will decrease by 0.0001083.

Table 9: R value, R square value, regression model and their respective interpretations for *STEC* exposed to winter sunlight and darkness taken from phase 2 data

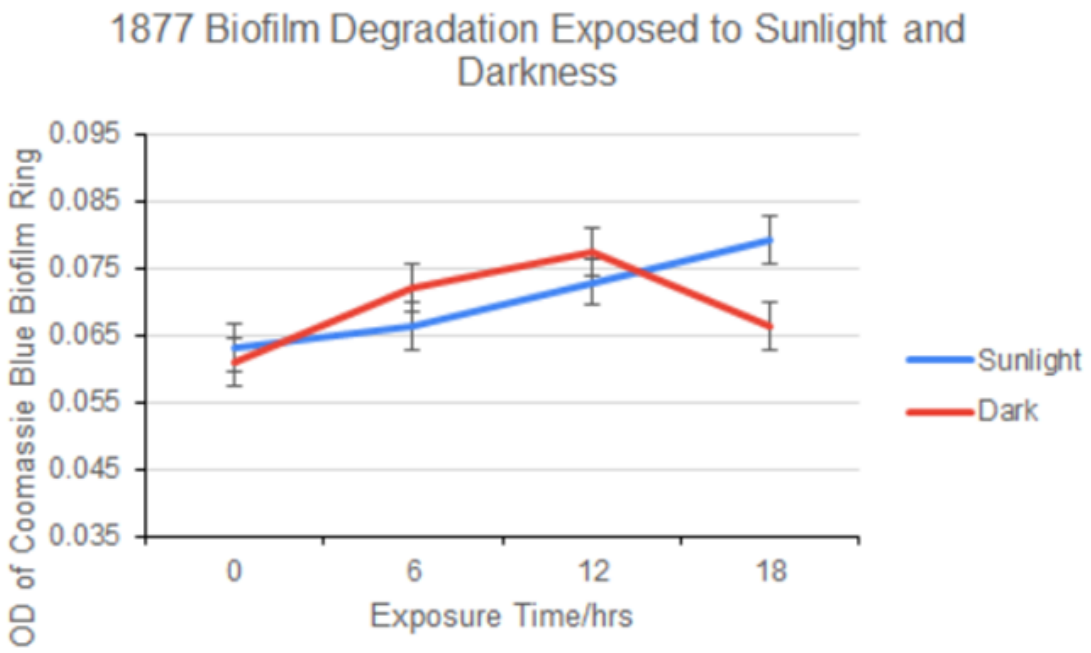

Figure 4.7: Graphical representation of OD of CBB G-250 stained biofilm rings of *Vibrio 1877* after biofilm degradation in sunlight and in darkness taken from phase 2 data. X axis represents the exposure time in hours and Y axis represents OD of coomassie blue stained biofilm rings

Organism	R value and interpretation	R2 value and interpretation	Regression model and interpretation
1877 SUNLIGHT	0.9905 Strong Positive Correlation	R2 = 0.9811 98.11% of the total variation of OD of biofilm stain OD can be explained by the regression model.	y =0.062325 + 0.0009083x When the time of exposure is 0 hour, the OD of biofilm stain will be 0.062325. And when time of exposure increases by 1 hour, OD of biofilm stains will increase by 0.0009083.
1877 DARK	0.3846 Weak Positive Correlation	R2 = 0.0148 14.79% of the total variation of OD of biofilm stain OD can be explained by the regression model.	y = 0.066 + 0.0003542x When time of exposure is 0 hour, the OD of biofilm stain will be 0.066. And when time of exposure increases by 1 hour, OD of biofilm stains will increase by 0.0003542.

Table 10: R value, R square value, regression model and their respective interpretations for *Vibrio 1877* exposed to winter sunlight and darkness taken from phase 2 data

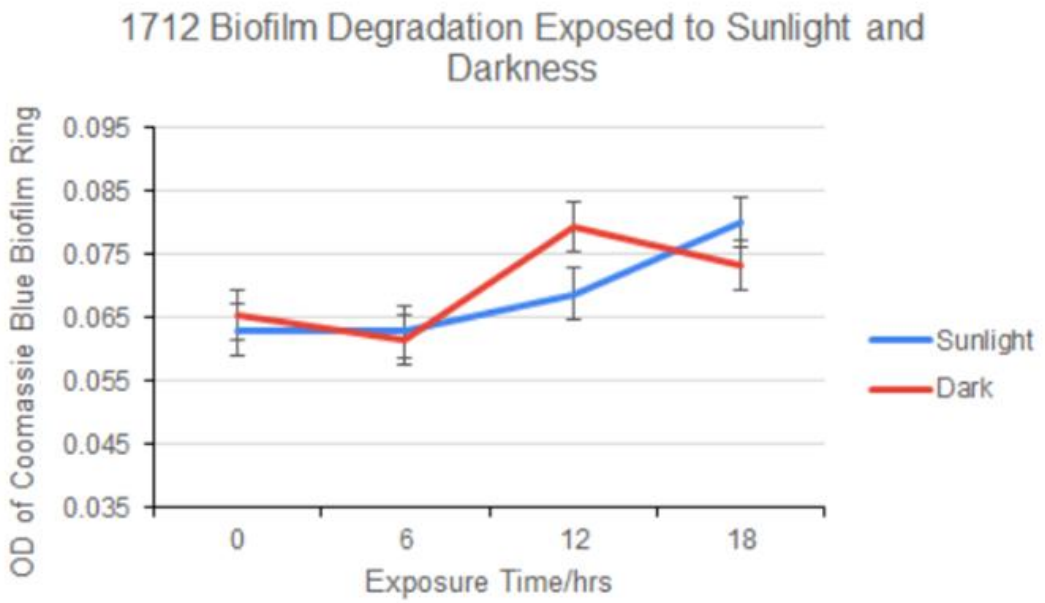

Figure 4.8: Graphical representation of OD of CBB G-250 stained biofilm rings of *Vibrio 1712* after biofilm degradation in sunlight and in darkness taken from phase 2 data. X axis represents the exposure time in hours and Y axis represents OD of coomassie blue stained biofilm rings

Organism	R value and interpretation	R2 value and interpretation	Regression model and interpretation
1712 SUNLIGHT	0.9114 Strong Positive Correlation	R2 = 0.8307 83.07% of the total variation of OD of biofilm stain OD can be explained by the regression model.	y = 0.060075 + 0.00095x When time of exposure is 0 hour, the OD of biofilm stain will be 0.060075. And when time of exposure will increase by 1 hour, OD of biofilm stains will increase by 0.00095.
1712 DARK	0.6676 Moderate Positive Correlation	R2 = 0.4457 44.57% of the total variation of OD of biofilm stain OD can be explained by the regression model.	y = 0.063725 + 0.0006833x When the time of exposure is 0 hour, the OD of biofilm stains will be 0.0623725. And when time of exposure increases by 1 hour, OD of biofilm stains will increase by 0.0006833.

Table 11: R value, R square value, regression model and their respective interpretations for *Vibrio 1712* exposed to winter sunlight and darkness taken from phase 2 data

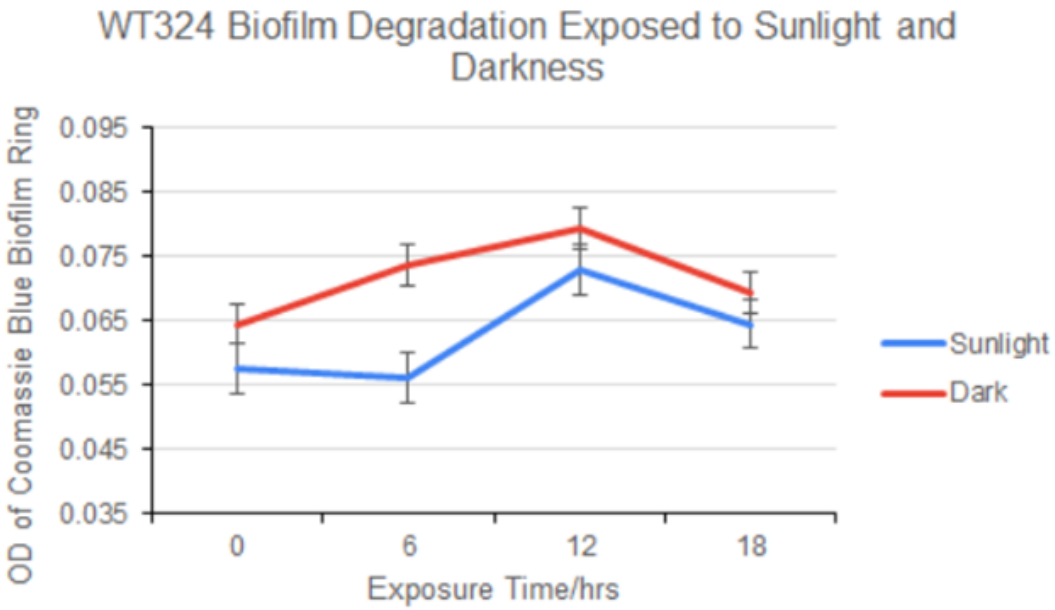

Figure 4.9: Graphical representation of OD of CBB G-250 stained biofilm rings of *Vibrio WT324* after biofilm degradation in sunlight and in darkness taken from phase 2 data. X axis represents the exposure time in hours and Y axis represents OD of coomassie blue stained biofilm rings

Organism	r value and interpretation	R2 value and interpretation	Regression model and interpretation
WT324 SUNLIGHT	0.6311 Moderate Positive Correlation	R2 = 0.3983 39.83% of the total variation of OD of biofilm stain OD can be explained by the regression model.	y = 0.05705 + 0.0006333x When the time of exposure is 0 hour, the OD of biofilm stain will be 0.05705. And when time of exposure increases by 1 hour, OD of biofilm stains will increase by 0.0006333.
WT324 DARK	0.4034 Moderate Positive Correlation	R2 = 0.1628 16.28% of the total variation of OD of biofilm stain OD can be explained by the regression model.	y = 0.06875 + 0.0003333x When the time of exposure is 0 hour, the OD of the biofilm stain will be 0.06875. And when time of exposure increases by 1 hour, OD of biofilm stains will increase by 0.0003333.

Table 12: R value, R square value, regression model and their respective interpretations for *Vibrio WT324* exposed to winter sunlight and darkness taken from phase 2 data

4.2.3 T-TESTS FOR OPTICAL DENSITY OF BIOFILM RINGS STAINED BY COOMASSIE BLUE

Null Hypothesis: There is no significant difference between OD of coomassie rings in winter sun and winter dark

Alternative Hypothesis: There is a significant difference between OD of coomassie rings in winter sun and winter dark

ORGANISM	Time/hour	p-value	Interpretation	NULL HYPOTHESIS	Overall remarks
STEC SUN VS. STEC DARK	0	0.8900	0.89 > 0.05	ACCEPT	NULL HYPOTHESIS IS ACCEPTED
	6	0.5900	0.59 > 0.05	ACCEPT	
	12	0.1400	0.14 > 0.05	ACCEPT	
	18	0.0800	0.080 > 0.05	ACCEPT	
1877 SUN VS. 1877 DARK	0	0.7900	0.79 > 0.05	ACCEPT	NULL HYPOTHESIS IS ACCEPTED
	6	0.3900	0.39 > 0.05	ACCEPT	
	12	0.7100	0.71 > 0.05	ACCEPT	
	18	0.3800	0.38 > 0.05	ACCEPT	
1712 SUN VS. 1712 DARK	0	0.8200	0.82 > 0.05	ACCEPT	NULL HYPOTHESIS IS ACCEPTED
	6	0.8300	0.83 > 0.05	ACCEPT	
	12	0.0048	0.0048 < 0.05	REJECT	
	18	0.7000	0.70 > 0.05	ACCEPT	
WT324 SUN VS. WT324 DARK	0	0.2800	0.28 > 0.05	ACCEPT	NULL HYPOTHESIS IS ACCEPTED
	6	0.0420	0.042 < 0.05	REJECT	
	12	0.6700	0.67 > 0.05	ACCEPT	
	18	0.5900	0.59 > 0.05	ACCEPT	

Table 13: Statistical significance comparison between the OD of coomassie blue stained biofilm rings taken from phase 2 data of biofilms exposed to winter sunlight and winter darkness by T-test

4.2.4 Interpretation of the Statistical Analysis of Phase 2 Data

According to the graphical representations, the optical density of the biofilm rings stained and then dissolved by glacial acetic acid increases with time in both sunlight exposure and the dataset that was kept in the dark *(Fig.4.6-Fig.4.9)*. During the 18 hour exposure time, the OD increased from the starting point for both the sunlight and dark data set. The increasing OD indicates that the thickness of the biofilm rings increases after they have been exposed to sunlight or darkness periodically every 6 hours. This increase is corroborated by the r value which shows weak to strong positive correlation between OD and the exposure time with the exception of *STEC* biofilm that was kept in the dark which shows weak negative correlation showing that the OD does not increase with exposure time i.e., the biofilm ring does not get thicker. The regression models give quantitative values of the OD increase with each hour increase in exposure time. These values are: 0.0007083 and 0.0001083 in sunlight and darkness respectively for *STEC*, 0.0009083 and 0.0003542 in sunlight and darkness respectively for *Vibrio 1877*, 0.00095 and 0.0006833 in sunlight and darkness respectively for *Vibrio 1712*, 0.0006333 and 0.0003333 in sunlight and darkness respectively for *Vibrio WT324 (Table 9-12)*. This shows that exposure to sunlight does not break the bacterial biofilm rings as the biofilm rings do not get thinner and the OD of the CBB G250 stain of these rings does not decrease. The increases look very insignificant which is again corroborated by the t-tests. Even though the graphical representation and the regression model shows that the OD increases in the data set that was exposed to sunlight, a t-test was done to show the level of significance for this increase. According to the t-tests, there is no significant difference between the OD of the biofilm stains exposed to sunlight and the ones kept in darkness during the winter season *(Table 13)*. This conclusively shows that the sunlight does not significantly break the bacterial biofilm rings to decrease its thickness during the winter season.

4.3.1 PHASE 3: Biofilm Formed on Coverslips

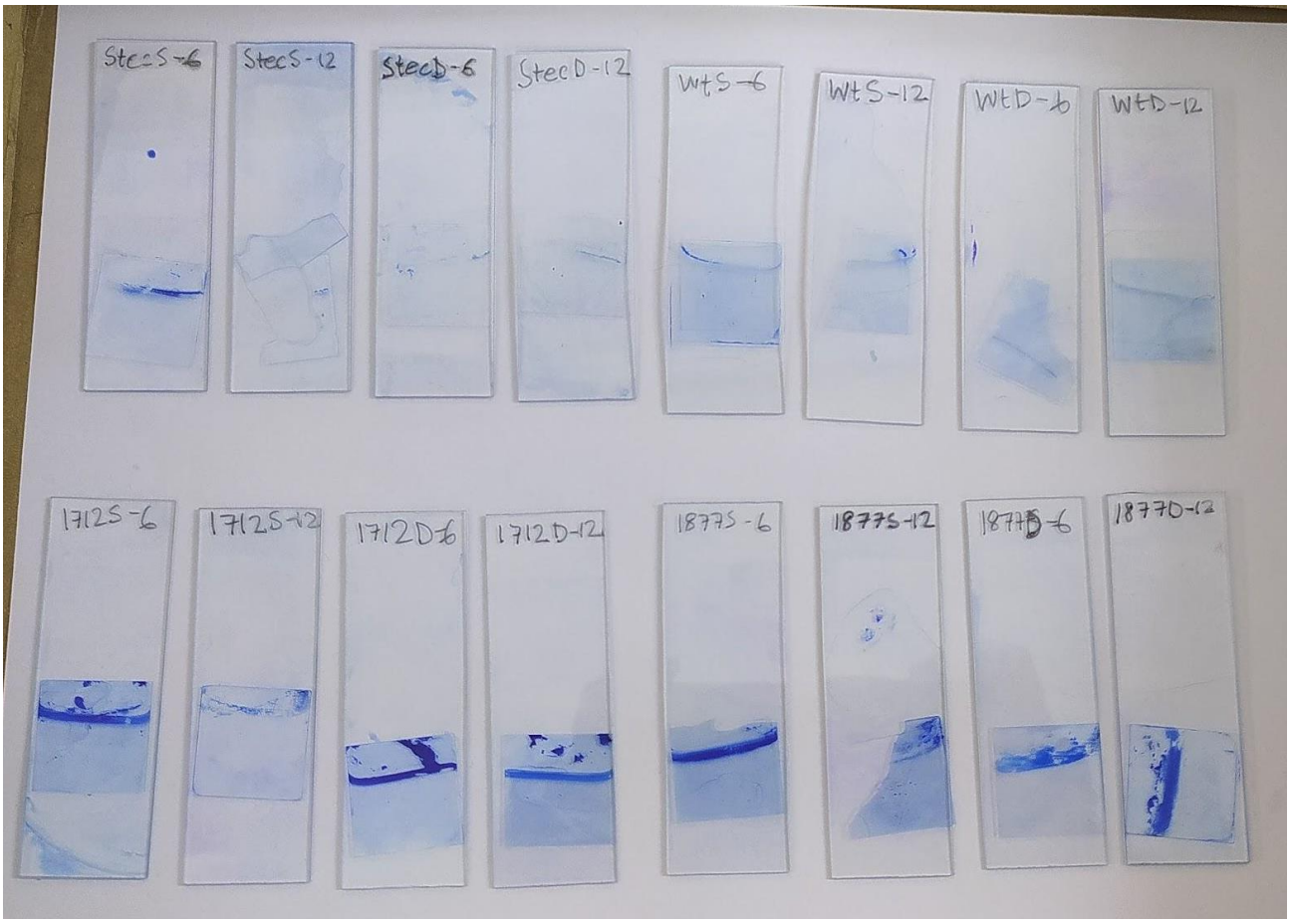

Figure 4.10: **Stained biofilms formed on the coverslips**. 'S' depicts the coverslips were exposed to the sunlight and 'D' depicts the coverslips were kept in the dark. '6' and '12' depict the number of hours the coverslips were exposed to the sunlight or kept in the dark. For instance, '1712S-6' shows the state of the biofilm formed by the stain after *Vibrio 1712* was exposed to 6 hours of sunlight. On the other hand, '1712D-6' indicates the state of biofilm formed by the stain after *Vibrio 1712* was kept in the dark for 6 hours.

4.3.2 Phase 3 Graphs and Regression Analysis

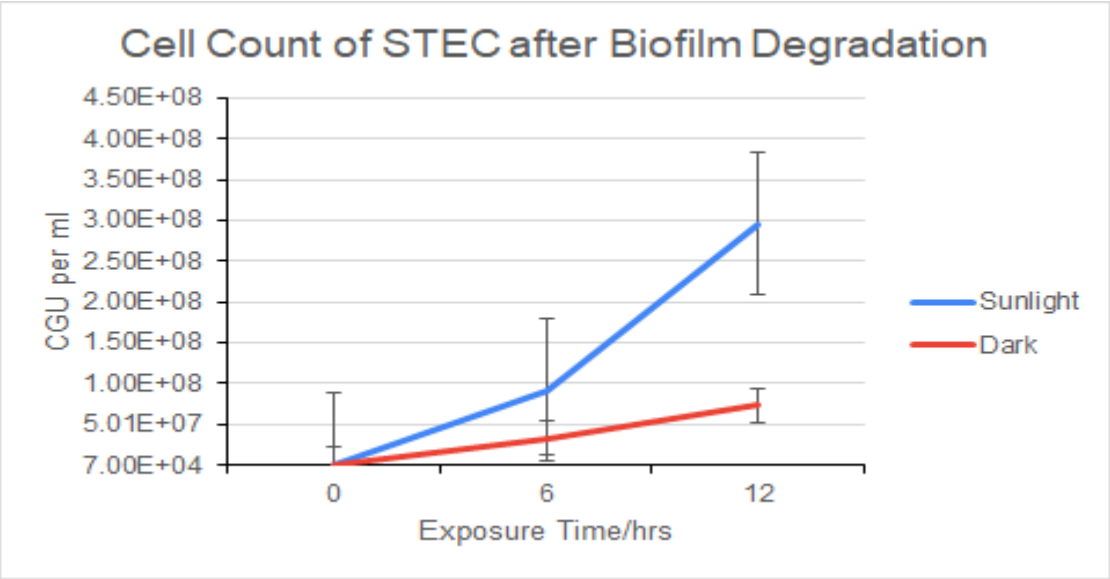

Figure 4.11: Graphical representation of cell count of *STEC* after biofilm degradation in sunlight and in darkness taken from phase 3 data. X axis represents the exposure time in hours and Y axis represents CFU per ml

Organism	r value and interpretation	R2 value and interpretation	Regression model and interpretation
STEC SUNLIGHT	0.9764 Strong Positive Correlation	R2 = 0.9535 95.35% of the total variation of the cell count can be explained by the regression model.	y = -1.84E+07 + 2.46E+07x When time of exposure in sunlight is 0 hour, cell count will be 1.84E+07 CFU/ml. And when time of exposure will increase by 1 hour, cell count will increase by 2.46E+07 CFU/ml.
STEC DARK	0.9979 Strong Positive Correlation	R2 = 0.9958 99.58% of the total variation of the cell count can be explained by the regression model	y = -1.30E+06 + 6.09E+06x When time of exposure in the dark is 0, cell count will be 1.30E+06 CFU/ml. And when time of exposure will increase by 1 hour, cell count will increase by 6.09E+06 CFU/ml.

Table 14: R value, R square value, regression model and their respective interpretations for *STEC* exposed to winter sunlight and darkness taken from phase 3 data

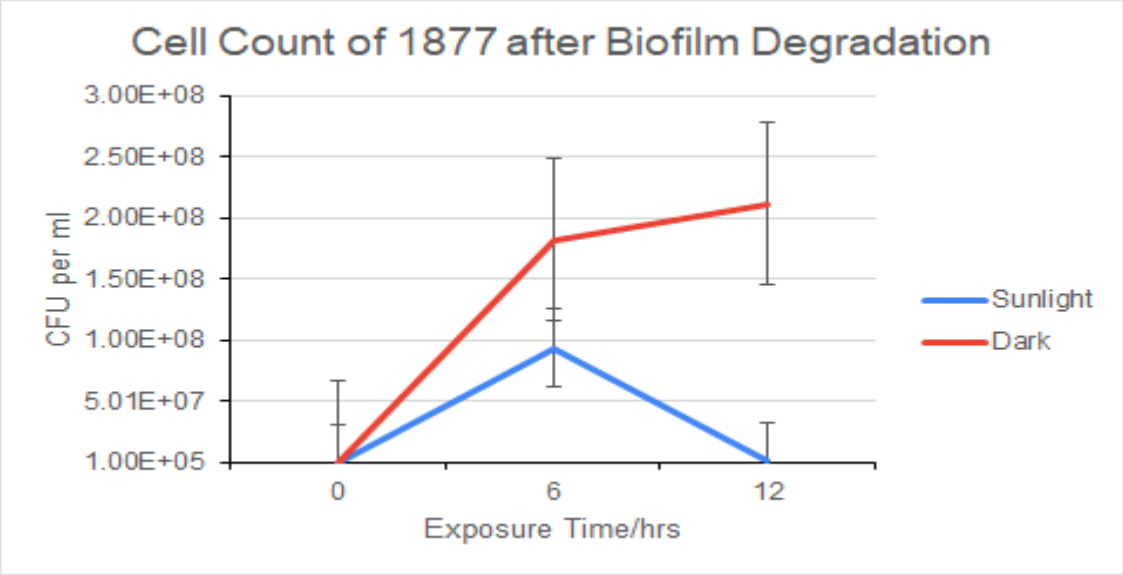

Figure 4.12: Graphical representation of cell count of *Vibrio 1877* after biofilm degradation in sunlight and in darkness taken from phase 3 data. X axis represents the exposure time in hours and Y axis represents CFU per ml

Organism	r value and interpretation	R2 value and interpretation	Regression model and interpretation
1877 SUNLIGHT	0.0064 No Correlation	R2 = 0.00 0% of the total variation of the cell count can be explained by the regression model.	y = 3.14E+07 + 5.71E+04x When time of exposure in sunlight is 0 hour, cell count will be 3.14E+07 CFU/ml. And when time of exposure will increase by 1 hour, cell count will increase by 5.71E+04 CFU/ml.
1877 DARK	0.9226 Strong Positive Correlation	R2 = 0.8511 85.11% of the total variation of the cell count can be explained by the regression model	y = 2.56E+07 + 1.76E+07x When time of exposure in the dark is 0 hour, cell count will be 2.56E+07 CFU.ml. And when time of exposure increases by 1 hour, cell count will increase by 1.76E+07CFU/ml.

Table 15: R value, R square value, regression model and their respective interpretations for *Vibrio 1877* exposed to winter sunlight and darkness taken from phase 3 data

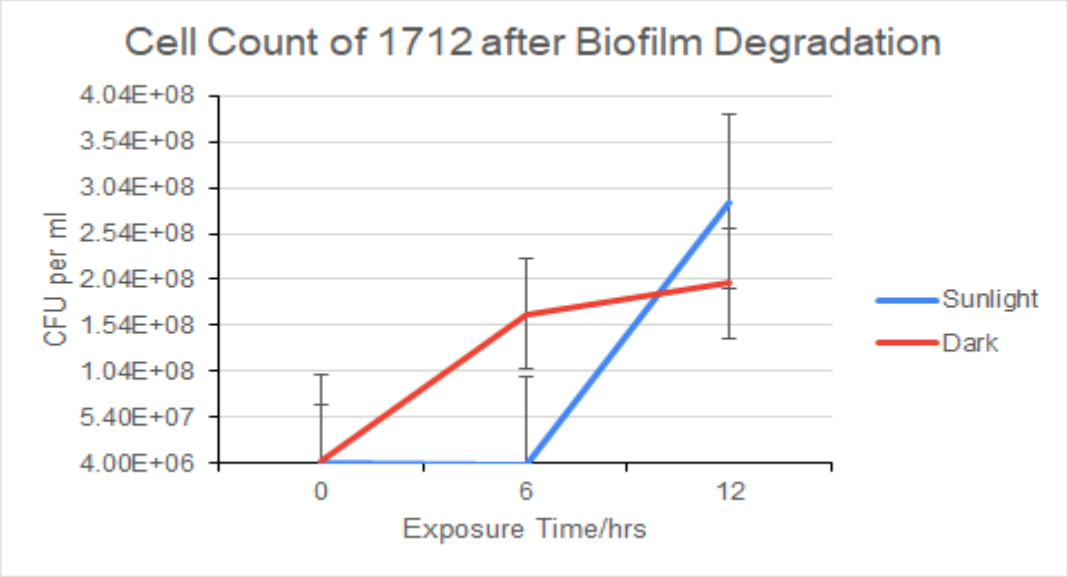

Figure 4.13: Graphical representation of cell count of *Vibrio 1712* after biofilm degradation in sunlight and in darkness taken from phase 3 data. X axis represents the exposure time in hours and Y axis represents CFU per ml

Organism	r value and interpretation	R2 value and interpretation	Regression model and interpretation
1712 SUNLIGHT	0.8628 Strong Positive Correlation	R2 = 0.7445 74.45% of the total variation of the cell count can be explained by the regression model.	y = -4.41E+07 + 2.37E+07x When time of exposure in sunlight is 0 hour, cell count will be -4.41E+07 CFU/ml. And when time of exposure will increase by 1 hour, cell count will increase by 2.37E+07 CFU/ml.
1712 DARK	0.9357 Strong Positive Correlation	R2 = 0.8756 87.56% of the total variation of the cell count can be explained by the regression model	y = 2.80E+07 + 1.61E+07x When time of exposure in the dark is 0 hour, cell count will be 2.80E+07 CFU/ml. And when time of exposure will increase by 1 hour, cell count will increase by 1.61E+07 CFU/ml.

Table 16: R value, R square value, regression model and their respective interpretations for *Vibrio 1712* exposed to winter sunlight and darkness taken from phase 3 data

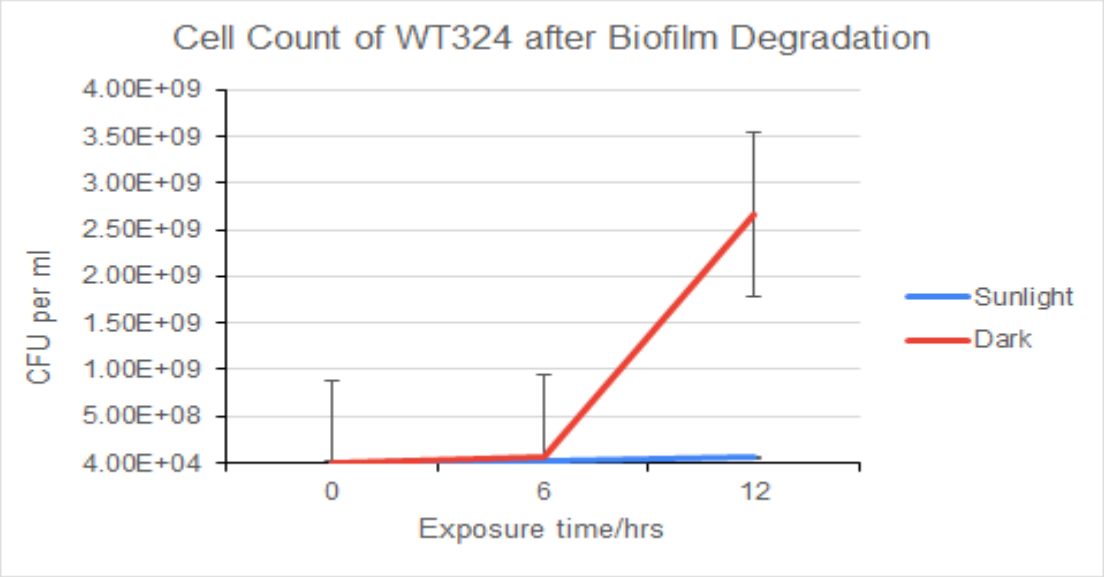

Figure 4.14: Graphical representation of cell count of *Vibrio WT324* after biofilm degradation in sunlight and in darkness taken from phase 3 data. X axis represents the exposure time in hours and Y axis represents CFU per ml

Organism	r value and interpretation	R2 value and interpretation	Regression model and interpretation
WT324 SUNLIGHT	0.9967 Strong Positive Correlation	R2 = 0.9933 99.33% of the total variation of the cell count can be explained by the regression model.	y = 6.97E+04 + 4.53E+06x When time of exposure in sunlight is 0 hour, cell count will be 6.97E+04 CFU/ml. And when time of exposure will increase by 1 hour, cell count will increase by 4.53E+06 CFU/ml.
WT324 DARK	0.8760 Strong Positive Correlation	R2 = 0.7673 76.73% of the total variation of the cell count can be explained by the regression model	y = -4.21E+08 + 2.22E+08x When time of exposure in the dark is 0 hour, cell count will be 4.21E+08 CFU/ml. And when time of exposure will increase by 1 hour, cell count will increase by 2.22E+08 CFU/ml.

Table 17: R value, R square value, regression model and their respective interpretations for *Vibrio WT324* exposed to winter sunlight and darkness taken from phase 3 data

4.3.3 T-TEST RESULTS FOR BIOFILMS FORMED ON COVERSLIPS

Null Hypothesis: There is no significant difference between cell count in winter sun and winter dark

Alternative Hypothesis: There is a significant difference between cell count in winter sun and winter dark

ORGANISM	Time/hour	p-value	Interpretation	NULL HYPOTHESIS	Overall remarks
STEC SUN VS. STEC DARK	0	0.35	0.35 > 0.05	ACCEPT	NULL HYPOTHESIS IS ACCEPTED
	6	0.56	0.56 > 0.05	ACCEPT	
	12	0.44	0.44 > 0.05	ACCEPT	
1877 SUN VS. 1877 DARK	0	0.35	0.35 > 0.05	ACCEPT	NULL HYPOTHESIS IS ACCEPTED
	6	0.65	0.65 > 0.05	ACCEPT	
	12	0.019	0.019 < 0.05	REJECT	
1712 SUN VS. 1712 DARK	0	0.70	0.70 > 0.05	ACCEPT	NULL HYPOTHESIS IS ACCEPTED
	6	0.12	0.12 > 0.05	ACCEPT	
	12	0.68	0.68 > 0.05	ACCEPT	
WT324 SUN VS. WT324 DARK	0	0.38	0.38 > 0.05	ACCEPT	NULL HYPOTHESIS IS ACCEPTED
	6	0.40	0.40 > 0.05	ACCEPT	
	12	0.36	0.36 > 0.05	ACCEPT	

Table 18: Statistical Significance Comparison between the Cell Count Taken from Phase 3 Data of Biofilms Exposed to Winter Sunlight and Winter Darkness By T-test

4.3.4 Interpretation of the Statistical Analysis of Phase 3 Data

According to the graphical representations, the cell count increases with time in both sunlight exposure and the dataset that was kept in the dark *(Fig.4.11, 4.13, 4.14)*, with the exception of *Vibrio 1877 (Fig. 4.12)*, where the cell count decreased in the second 6 hours for the data set that was exposed to sunlight. The increase in cell count with time is corroborated by the r value which shows strong positive correlation between cell count and the exposure time with the exception of the *Vibrio 1877* data set that was exposed to sunlight that shows no correlation between the cell count and exposure time. The regression models give quantitative values of how the cell count will increase with each hour increase in exposure time. These values are: 2.46E+07 CFU/ml and 6.09E+06 CFU/ml in sunlight and darkness respectively for *STEC*, 5.71E+04 CFU/ml and 1.76E+07 CFU/ml in sunlight and darkness respectively for *Vibrio 1877*, 2.37E+07 CFU/ml and 1.61E+07 CFU/ml in sunlight and darkness respectively for *Vibrio 1712*, 4.53E+06 CFU/ml and

2.22E+08 CFU/ml in sunlight and darkness respectively for *Vibrio WT324*. However, even though the graphical representation and the regression model shows that the cell count increases in the data set that was exposed to sunlight, a t-test was done to show the level of significance for this increase *(Table 14-17)*. According to the t-tests, there is no significant difference between the cell count of the biofilms exposed to sunlight and the ones kept in darkness during the winter season *(Table 18)*. This conclusively shows that the sunlight does not significantly break the bacterial biofilms to resuscitate a significant amount of planktonic bacteria during the winter season.

4.4.1 PHASE 4: OD of biofilm formed in ELISA plates

4.4.2 Phase 4 Graphs and Regression Analysis

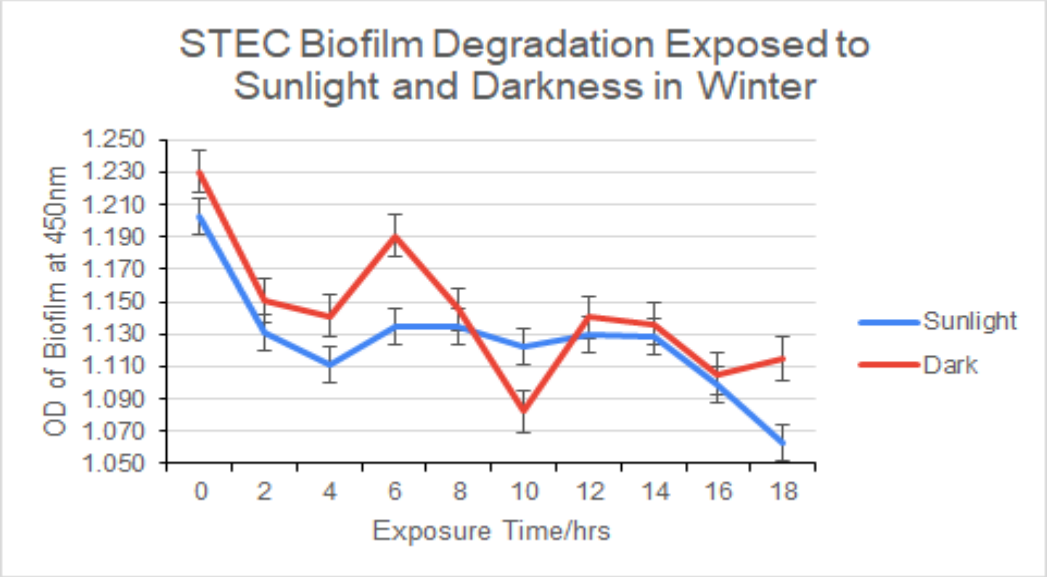

Figure 4.15: Graphical representation of OD of biofilms formed in 96-well ELISA plate of *STEC* after biofilm degradation in sunlight and in darkness taken from phase 4 data. X axis represents the exposure time in hours and Y axis represents OD of the biofilm

Organism	R value and Interpretation	R2 value and Interpretation	Regression model and Interpretation
STEC SUNLIGHT	-0.7466 Weak Negative Correlation	R2 = 0.5574 55.74% of the variation in OD of STEC biofilm can be explained by the time of exposure in sun	y = 1.164503 - 0.0043202x When time of exposure is 0 hour, the OD of biofilm will be 1.164503. And when time of exposure increases by 1 hour, OD of biofilm will decrease by 0.0043202.
STEC DARK	-0.6975 Moderate Negative Correlation	R2 = 0.4865 48.65% of the variation in OD of STEC biofilm can be explained by the time of exposure in the dark.	y = 1.18746 - 0.0048448x When the time of exposure is 0 hour, the OD of biofilm will be 1.18746. And when time of exposure increases by 1 hour, OD of biofilm will decrease by 0.0048448.

Table 19: R value, R square value, regression model and their respective interpretations for *STEC* exposed to winter sunlight and darkness taken from phase 4 data

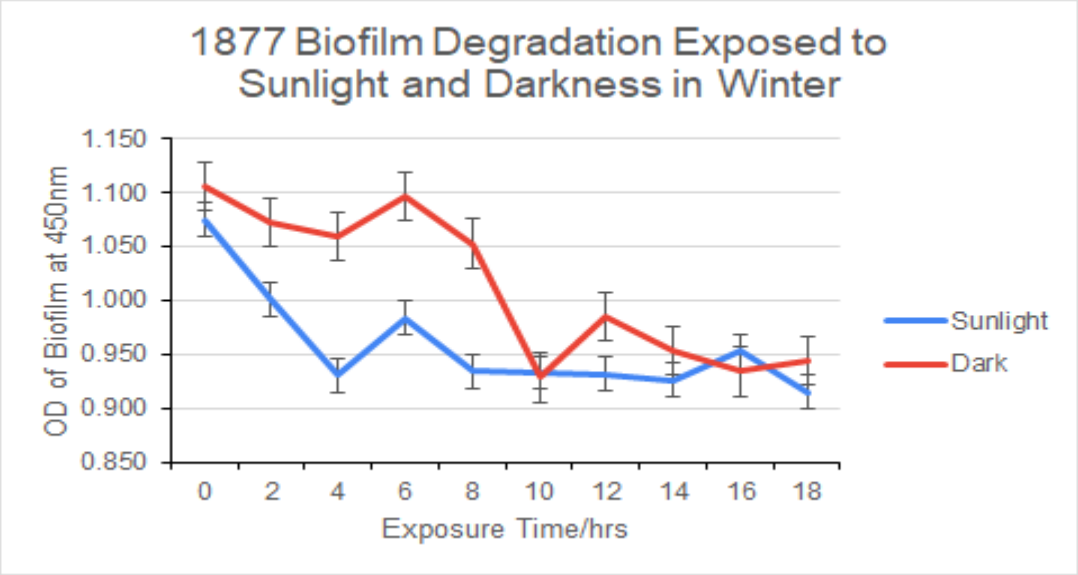

Figure 4.16: Graphical representation of OD of biofilms formed in 96 well ELISA plate of *Vibrio 1877* after biofilm degradation in sunlight and in darkness taken from phase 4 data. X axis represents the exposure time in hours and Y axis represents OD of the biofilm

Organism	R value and interpretation	R2 value and interpretation	Regression model and interpretation
1877 SUNLIGHT	-0.73 Strong Negative Correlation	R2 = 0.5329 53.29% of the variation in OD of 1877 biofilm can be explained by the time of exposure in the sun.	y = 1.011515 - 0.058918x When the time of exposure is 0 hour, the OD of biofilm will be 1.011515. And when time of exposure will increase by 1 hour, OD of biofilm will decrease by 0.058918.
1877 DARK	-0.8833 Strong Negative Correlation	R2 = 0.7803 78.03% of the variation in OD of STEC biofilm can be explained by the time of exposure in the dark.	y = 1.106648 - 0.0103678x When the time of exposure is 0 hour, the OD of biofilm will be 1.106648. And when time of exposure increases by 1 hour, OD of biofilm will decrease by 0.0103678.

Table 20: R value, R square value, regression model and their respective interpretations for *Vibrio 1877* exposed to winter sunlight and darkness taken from phase 4 data

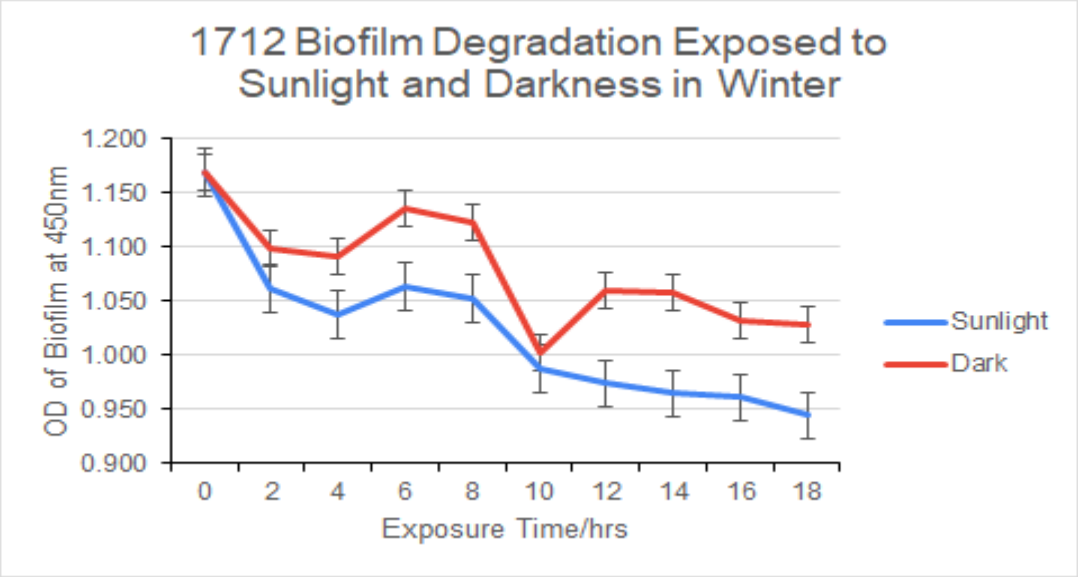

Figure 4.17: Graphical representation of OD of biofilms formed in 96 well ELISA plate of *Vibrio 1712* after biofilm degradation in sunlight and in darkness taken from phase 4 data. X axis represents the exposure time in hours and Y axis represents OD of the biofilm

Organism	R value and interpretation	R2 value and interpretation	Regression model and interpretation
1712 SUNLIGHT	-0.9129 Strong Negative Correlation	R2 = 0.8334 83.34% of the variation in OD of 1877 biofilm can be explained by the time of exposure in the sun.	y = 1.114857 - 0.0103947x When time of exposure is 0 hour, the OD of biofilm will be 1.114857. And when time of exposure increases by 1 hour, OD of biofilm will decrease by 0.0103947.
1712 DARK	-0.783 Strong Negative Correlation	R2 = 0.6131 61.31% of the variation in OD of STEC biofilm can be explained by the time of exposure in the dark.	y = 1.14146 - 0.0068548x When the time of exposure is 0 hour, the OD of biofilm will be 1.14146. And when time of exposure increases by 1 hour, OD of biofilm will decrease by 0.0068548.

Table 21: R value, R square value, regression model and their respective interpretations for *Vibrio 1712* exposed to winter sunlight and darkness taken from phase 4 data

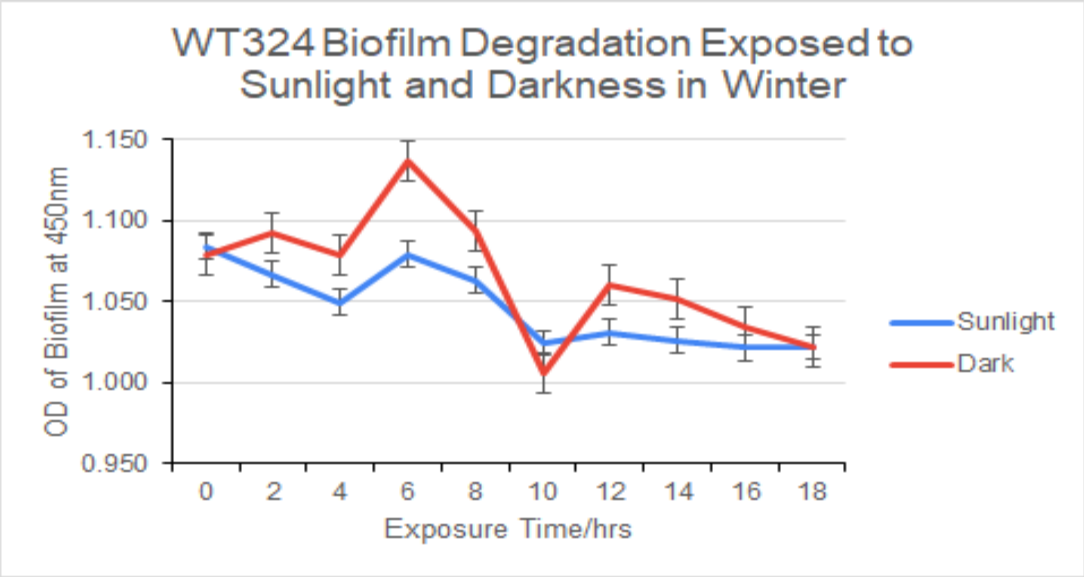

Figure 4.18: Graphical representation of OD of biofilms formed in 96 well ELISA plate of *Vibrio WT324* after biofilm degradation in sunlight and in darkness taken from phase 4 data. X axis represents the exposure time in hours and Y axis represents OD of the biofilm

Organism	R value and interpretation	R2 value and interpretation	Regression model and interpretation
WT324 SUNLIGHT	-0.8695 Strong Negative Correlation	R2 = 0.7560 75.60% of the variation in OD of 1877 biofilm can be explained by the time of exposure in the sun.	y = 1.078718 - 0.0035676x When the time of exposure is 0 hour, the OD of biofilm will be 1.078718. And when time of exposure increases by 1 hour, OD of biofilm will decrease by 0.003567.
WT324 DARK	-0.6476 Moderate Negative Correlation	R2 = 0.4194 41.94% of the variation in OD of STEC biofilm can be explained by the time of exposure in the dark.	y = 1.102686 - 0.0041454x When the time of exposure is 0 hour, the OD of biofilm will be 1.102686. And when time of exposure increases by 1 hour, OD of biofilm will decrease by 0.0041454.

Table 22: R value, R square value, regression model and their respective interpretations for *Vibrio WT324* exposed to winter sunlight and darkness taken from phase 4 data

4.4.3 T-TESTS FOR BIOFILM OD TAKEN BY ELISA EXPOSED TO WINTER SUNLIGHT AND DARKNESS:

Null Hypothesis: There is no significant difference between OD of biofilm kept in winter sunlight and winter dark

Alternative Hypothesis: There is a significant difference in OD of biofilm kept in winter sunlight and winter dark

ORGANISM	Time/hour	p-value	Interpretation	NULL HYPOTHESIS	Overall remarks
STEC SUN VS. STEC DARK	0	0.600	0.60 > 0.05	ACCEPT	NULL HYPOTHESIS IS ACCEPTED
	6	0.240	0.24 > 0.05	ACCEPT	
	12	0.890	0.89 > 0.05	ACCEPT	
	18	0.680	0.68 > 0.05	ACCEPT	
1877 SUN VS. 1877 DARK	0	0.450	0.45 > 0.05	ACCEPT	NULL HYPOTHESIS IS ACCEPTED
	6	0.044	0.044 < 0.05	REJECT	
	12	0.400	0.40 > 0.05	ACCEPT	
	18	0.560	0.56 > 0.05	ACCEPT	
1712 SUN VS. 1712 DARK	0	0.990	0.99 > 0.05	ACCEPT	NULL HYPOTHESIS IS ACCEPTED
	6	0.340	0.34 > 0.05	ACCEPT	
	12	0.190	0.19 > 0.05	ACCEPT	
	18	0.360	0.36 > 0.05	ACCEPT	
WT324 SUN VS. WT324 DARK	0	0.950	0.95 > 0.05	ACCEPT	NULL HYPOTHESIS IS ACCEPTED
	6	0.360	0.36 > 0.05	ACCEPT	
	12	0.700	0.70 > 0.05	ACCEPT	
	18	0.990	0.99 > 0.05	ACCEPT	

Table 23: Statistical Significance Comparison Between The OD Of Biofilms That Were Formed On 96 Well Elisa Plates Taken From Phase 4 Data Of Biofilms Exposed To Winter Sunlight And Winter Darkness By T-test

4.4.4 Interpretation of the Statistical Analysis of Phase 4 Data

According to the graphical representations, the optical density of the biofilms in a 96 well ELISA plate decreases with time in both sunlight exposure and the dataset that was kept in the dark *(Fig. 4.15-Fig.4.18)*. During the 18 hour exposure time, the OD decreased from the starting point for both the sunlight and dark data set. This decrease is corroborated by the r value which shows weak to strong negative correlation between OD and the exposure time showing that the OD decreases with exposure time. This means that exposure to sunlight breaks bacterial biofilms in the ELISA plates and as a result the optical density decreases. The regression models give quantitative values of how much the OD will decrease with each hour increase in exposure time. These values are: 0.0043202 and 0.0048448 in sunlight and darkness respectively for *STEC*, 0.058918 and 0.0103678 in sunlight and darkness respectively for *Vibrio 1877*, 0.0103947 and 0.0068548 in sunlight and darkness respectively for *Vibrio 1712*, 0.003567 and 0.0041454 in sunlight and darkness respectively for *Vibrio WT324 (Table19-22)*. However, these decreases look very insignificant which is again corroborated by the t-tests. Along with the graphical representation and the regression model showing that the OD decreases in the data set that was exposed to sunlight, a t-test was done to show the level of significance for this decrease. According to the t-tests, there is no significant difference between the OD of the biofilms exposed to sunlight and the ones kept in darkness during the winter season *(Table 23)*. This conclusively shows that the sunlight does not significantly break the bacterial biofilm to resuscitate a significant amount of planktonic bacteria during the winter season.

4.5.1 Comparison between the Data of Biofilms Exposed to Sunlight in Summer and Winter

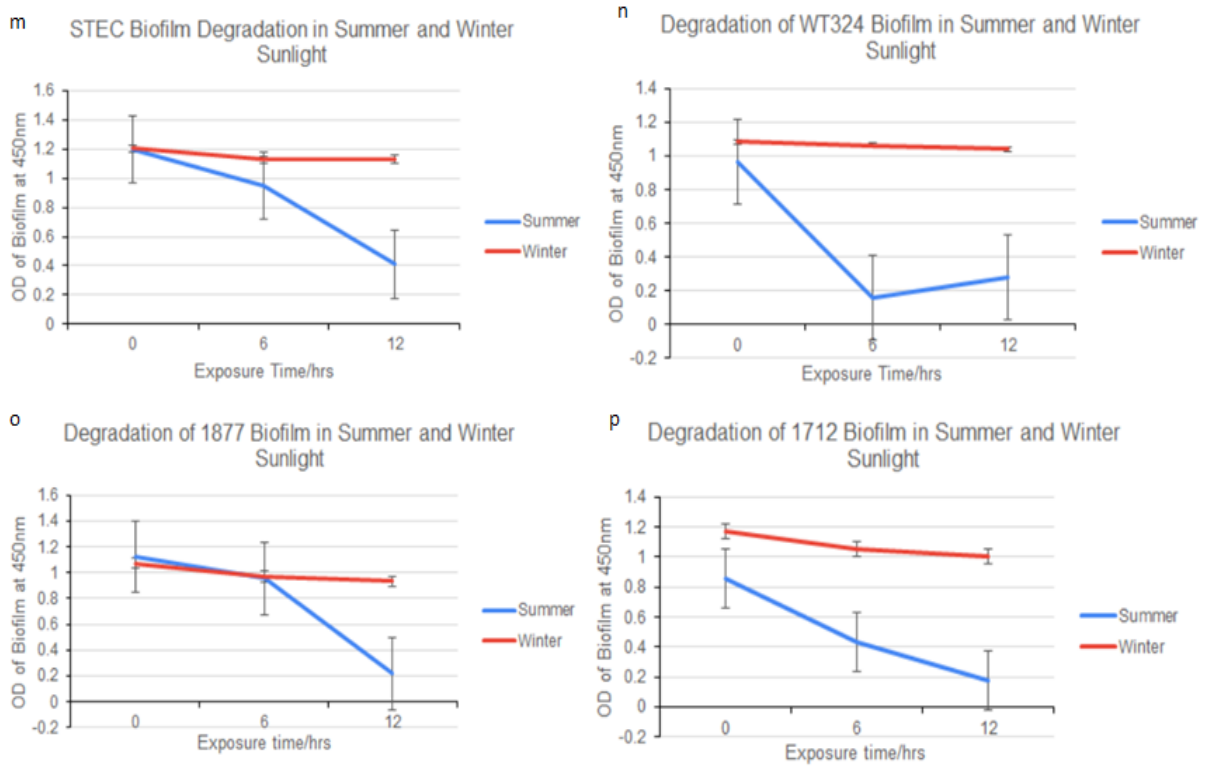

Figure 4.19: **The image depicts the changes in OD of 4 different bacterial strains exposed to sunlight over a period of 12 hours in summer and winter, where the biofilms were formed on 96-well ELISA plates**. Image (m) shows the changes in OD obtained after exposing *STEC* biofilm to 12 hours of sunlight in summer and winter. Similarly, image (o) shows the changes obtained after exposing *1877 Vibrio*, image (p) from *1712 Vibrio*, and finally, image (n) from *WT324 Vibrio*. Here the X axis represents the exposure time in hours in sunlight and the Y axis represents the optical density (OD) of biofilms at 450 nm wavelength.

4.5.2 T-TESTS FOR COMPARISON BETWEEN OD OF BIOFILMS THAT WERE FORMED IN 96-WELL ELISA PLATES EXPOSED TO SUNLIGHT IN SUMMER SEASON AND SUNLIGHT IN WINTER SEASON

Null Hypothesis: There is no significant difference between OD of biofilm exposed to summer sun and winter sun

Alternative Hypothesis: There is a significant difference between OD of biofilm exposed to summer sun and winter sun

ORGANISM	Time/hour	p-value	Interpretation	NULL HYPOTHESIS	Overall remarks
Summer STEC Sun Vs Winter STEC Sun	0	0.0110000	0.011 < 0.05	REJECT	NULL HYPOTHESIS IS REJECTED
	6	0.2800000	0.65 > 0.05	ACCEPT	
	12	0.0023000	0.0023 < 0.05	REJECT	
Summer 1877 Sun Vs Winter 1877 Sun	0	0.2200000	0.22 > 0.05	ACCEPT	NULL HYPOTHESIS IS ACCEPTED
	6	0.8100000	0.81 > 0.05	ACCEPT	
	12	0.0000032	0.0000032 < 0.05	REJECT	
Summer 1712 Sun Vs Winter 1712 Sun	0	0.0130000	0.013 < 0.05	REJECT	NULL HYPOTHESIS IS REJECTED
	6	0.0002300	0.00023 < 0.05	REJECT	
	12	0.0000120	0.000012 < 0.05	REJECT	
Summer WT324 Sun Vs Winter WT324 Sun	0	0.0013000	0.0013 < 0.05	REJECT	NULL HYPOTHESIS IS REJECTED
	6	0.0000870	0.000087 < 0.05	REJECT	
	12	0.0000140	0.000014 < 0.05	REJECT	

Table 24: Statistical Significance Comparison Between OD Of Biofilms That Were Formed On 96 Well Elisa Plates Exposed To Sunlight In Summer Season And Sunlight In Winter Season By T-test

4.5.3 Interpretation of the Graphical Representation and the T-test Comparing the Degradation of Biofilms by Summer Sunlight Exposure and Winter Sunlight Exposure:

The exposure of bacterial biofilms made in a 96 well ELISA plate to sunlight had shown some decrease in the optical density indicating that there is so much breakage of the biofilms due to sunlight in the winter season. However, comparing this breakage with the data from summer season shows just how insignificant the breakage was in winter. It can already be visualized from the graphical representation how much the OD decreases in the summer compared to winter. Sharp declines in OD can be visible in the 12 hour exposure of these bacterial biofilms to sunlight in the summer season while in winter the curves, though decline, are very steadily decreasing and almost

maintain a constant trait *(Fig.4.19)*. This again is corroborated by the t-tests that were done to compare the decrease in OD in summer as opposed to the decrease in OD in winter due to sunlight exposure. *STEC*, *Vibrio 1712* and *Vibrio WT324* all rejected the null hypothesis, indicating that there was significant difference between OD of biofilm exposed to sunlight in summer and OD exposed to sunlight in winter with the exception of *Vibrio 1877* that accepted the null hypothesis that there is no significant difference between OD of biofilm exposed to sunlight in summer and biofilms exposed to sunlight in winter *(Table 24)*. This means that the OD of the biofilms in summer decreased significantly more than the decrease in OD of the biofilms exposed to sunlight in the winter. As a result, it can be conclusively stated that, the breakage of bacterial biofilms in the summer season due to sunlight is much more significant that the breakage of bacterial biofilms due to sunlight in winter.

Chapter 5:

Discussion

In this study, the effect of winter sunlight on bacterial biofilm was investigated. *Vibrio cholerae* causes seasonal epidemic cycles in Bangladesh. Diseases like cholera and diarrhea or bloody diarrhea are more prominent in summer than in winter. These bacteria form biofilms and survive in the environment throughout the year. Previously, it was investigated and concluded that summer sunlight resuscitates the bacterial biofilm. Thus, this study investigates whether winter sunlight can also resuscitate the bacterial biofilm or not.

5.1 Key findings

In both phase 1 and phase 3, it was observed that the cell count of both sets exposed to sunlight and darkness increased with time of exposure. The data suggests an exception as cell count was observed to decrease after 6 hours of exposure for the strain *WT324 Vibrio* in phase 1 (vials) and *1877 Vibrio* in phase 3 (coverslips).

In phase 2, OD of biofilm rings dissolved using glacial acetic acid was observed to increase with time of exposure when exposed to sunlight and kept in the dark. This indicates the thickness of biofilm rings increased over 18 hours. The only exception observed was in the case of *STEC* biofilm that was kept in the dark, where the OD does not increase with exposure time.

In phase 4, OD of biofilms were observed to decrease with time of exposure when in both sunlight and dark data sets. The data found in this phase showed no cases of exceptions.

Comparing the winter sunlight and dark data sets using statistical analysis revealed there is no significant difference between the data obtained from sunlight exposure and the data obtained from darkness exposure. Thus, the results derived support the hypothesis that winter sunlight does not have a significant effect on the bacterial biofilm.

When the data from summer sunlight set and winter sunlight set is compared using statistical analysis, it is found that there is a significant difference between the data except for the strain *Vibrio 1877*. The graphs show a significant degradation of the biofilm in summer compared to winter, and the statistical analysis confirms the significance difference. Thus, summer sunlight significantly degrades the bacterial biofilm, causing bacteria to be motile unlike the winter sunlight.

5.2 Interpretations

5.2.1 *STEC*: According to data collected from phase 1 and 3, planktonic bacterial cell count was observed to increase in both data sets, sunlight and darkness exposure. The graphical representation showed a significant increase in cell count in the later 6 hours compared to the first 6 hours *(Fig:4.2 and Fig:4.11)*. A correlation analysis suggested a strong positive correlation between cell count and exposure time. Additionally, the regression analysis suggested 87.97% and 95.35% of total variation in sunlight data set in phase 1 and phase 3 data respectively, and 84.06% and 99.57% of total variation in dark data set from phase 1 and phase 3 respectively can be explained by the regression models *(Table 2 and Table 14)*. Even though the graph shows a difference in the rate of increase of cell count in the two data sets, t-test showed there are no significant differences between the two data sets *(Table 6 and Table 18)*. On the other hand, phase 2 data shows an increase in the optical density of coomassie stains that were used to stain the biofilm rings post exposure in the sunlight exposed data set and a net no difference in OD in the darkness exposed data set. The graphical representation showed a steady increase in OD of the biofilms that were exposed to sunlight *(Fig: 4.6)* indicating that the biofilm did not get thinner due to breakage when exposed to sunlight while the biofilms kept in the dark showed a decrease in OD in the second 6 hour exposure period but it got back up to the starting optical density in the third 6 hour exposure period. This decrease could be an anomaly caused by the usage of different vials and different initial biofilm ring thickness. This pattern shown through the graphical representation is also visible in the correlation analysis which suggested a strong positive correlation between OD and exposure time for the sunlight exposed dataset and a weak negative correlation between OD and exposure time for the darkness exposed dataset. Additionally, the regression analysis suggested 92.99% of total variation in both the sunlight and dark data sets can be explained by the regression models *(Table 9)*. However, even though the graph shows a difference in the rate of increase of OD in the two data sets, t-test showed there are no significant differences between the two data sets *(Table 13)*. Finally, phase 4 shows a decrease in the optical density of biofilms formed in an ELISA plate and exposed to sunlight and darkness. According to the graphical representation, the decline is sharpest during the first 4 hours and the last 2 hours of sunlight exposure with a stationary trend in the middle 10 hours of sunlight exposure *(Fig:4.15)*. While the correlation analysis showed a moderate to weak negative correlation between OD of biofilms and exposure time in sunlight and darkness respectively, the regression analysis suggested 55.74% and 48.65%

of total variation in both the sunlight and dark data sets respectively, can be explained by the regression models *(Table 19)*. However, even though the graph shows a difference in the rate of increase of OD in the two data sets, t-test showed there are no significant differences between the two data sets *(Table 23)*. Additionally, a comparison between the summer and winter data shows that the decrease in OD is much more significant in the summer compared to winter which can be seen in both the graphical representation *(Fig:4.19m)* and the t-test *(Table 24)*.

5.2.2 ***Vibrio 1877***: The data that was collected from phases 1 and 3 shows an increase and then a decrease in planktonic cell count with time for both sunlight and darkness exposure data sets. In the graphical representation, phase 1 shows a very slow increase in cell count due to sunlight exposure while phase 3 shows an increase in the first 6 hours of exposure and then a sharp decline in the next 6 hours *(Fig:4.3 and Fig:4.12)*. As a result, the net cell count does not seem to increase significantly. While, for both phases 1 and 3, the samples exposed to darkness show a sharp incline in cell count for the first 6 hours of exposure and then a sharp dip for phase 1 and a very slow rise in phase 3 in the next 6 hours. A correlation analysis suggested a strong positive correlation between cell count and exposure time with an exception of the phase 3 sunlight exposure data set which showed no correlation between cell count and exposure time. Additionally, the regression analysis suggested 75.03% and 0% of total variation in sunlight data set in phase 1 and phase 3 data respectively, and 0.005% and 85.11% of total variation in dark data set from phase 1 and phase 3 respectively can be explained by the regression models *(Table 3 and Table 15)*. Even though the graph shows a difference in the rate of increase of cell count in the two data sets, t-test showed there are no significant differences between the two data sets *(Table 6 and Table 18)*. Additionally phase 2 data showed an increase in the optical density of coomassie stains that were used to stain the biofilm rings post exposure in the sunlight exposed data set and a net no difference in OD in the darkness exposed data set. The graphical representation showed a very slow increase in OD of the biofilms that were exposed to sunlight indicating that the biofilm did not get thinner due to breakage when exposed to sunlight while the biofilms kept in the dark showed a decrease in OD in the last 6 hours of exposure period *(Fig:4.7)*. This pattern shown through the graphical representation is also visible in the correlation analysis which suggested a strong positive correlation between OD and exposure time for the sunlight exposed dataset and a weak positive correlation between OD and exposure time for the darkness exposed dataset. Additionally, the regression analysis suggested 98.11% and 14.79% of total variation in both the sunlight and dark

data sets respectively can be explained by the regression models *(Table 10)*. However, even though the graph shows a difference in the rate of increase of OD in the two data sets, t-test showed there are no significant differences between the two data sets *(Table 13)*. Finally, phase 4 shows a decrease in the optical density of biofilms formed in an ELISA plate and exposed to sunlight and darkness. According to the graphical representation, the decline is sharpest during the first 4 hours of sunlight exposure and then a very slow increase and decrease, maintaining a constant net OD for the rest of the 14 hours of exposure in the sunlight *(Fig:4.16).* While the correlation analysis showed a strong negative correlation between OD of biofilms and exposure time in sunlight and darkness, the regression analysis suggested 53.29% and 78.03% of total variation in both the sunlight and dark data sets respectively, can be explained by the regression models *(Table 20)*. However, even though the graph shows a difference in the rate of increase of OD in the two data sets, t-test showed there are no significant differences between the two data sets *(Table 23)*. Additionally, a comparison between the summer and winter data shows that the decrease in OD is much more significant in summer compared to winter which can be seen in both the graphical representation *(Fig:4.19o)* and the t-test *(Table 24)*.

5.2.3 ***Vibrio 1712***: According to data collected from phases 1 and 3, planktonic bacterial cell count was observed to increase in both data sets, sunlight and darkness exposure. In phase 1, the graphical representation showed a significant increase in cell count in the first 6 hours compared to the later 6 hours for the sunlight data set, and the opposite in the dark data set *(Fig:4.4)*. In phase 3, the graphical representation indicated the cell count remained almost constant for the first 6 hours, and drastically increased in the later 6 hours for the sunlight data set, whereas in the dark data set the increase in cell count was observed from the start *(Fig:4.13)*. A correlation analysis suggested a strong positive correlation between cell count and exposure time. Additionally, the regression analyses suggested 86.35% and 74.45% of total variation in sunlight data set in phase 1 and phase 3 data respectively, and 97.65 % and 87.56 % of total variation in dark data set from phase 1 and phase 3 respectively can be explained by the regression models *(Table 4 and Table 16)*. Regardless of the graphical representation, t-test showed there are no significant differences between the two data sets *(Table 6 and Table 18)*. On the other hand, phase 2 data shows an increase in the optical density of coomassie stains that were used to stain the biofilm rings post-exposure in both data sets. In the sunlight exposed data set, the graphical representation shows a steady increase, whereas in the darkness exposed data set, the OD is found to decrease in the first

6 hours, increase significantly in the next 6 hours and decrease again in 18 hours *(Fig:4.8)*. Thus, the data indicates the biofilm rings got thicker with exposure time in both data sets. This pattern shown through the graphical representation is also visible in the correlation analysis which suggested a strong positive correlation between OD and exposure time for the sunlight exposed dataset and a moderate positive correlation between OD and exposure time for the darkness exposed dataset. Additionally, the regression analysis suggested 83.07% of total variation in the sunlight data set and 44.57% in the dark data set can be explained by the regression models *(Table 11)*. Similar to the graphical representation, t-test showed there are no significant differences between the two data sets *(Table 13)*. Finally, phase 4 shows a decrease in the OD of biofilms formed in an ELISA plate when exposed to sunlight and darkness. According to the graphical representation, the OD steadily declined in the first 4 hours, and then was observed to increase in the next 2 hours. After 2 hours of steady decline, the sharpest decline was observed during 8-10 hours of exposure time in both data sets. In the sunlight exposed data set, the OD was found to increase in the next 2 hours but again started to steadily decline. For the darkness exposed data set, no increase in OD was observed after 10 hours, the OD continued to decline gradually *(Fig: 4.17)*. The correlation analysis showed a strong negative correlation between OD of biofilms and exposure time in sunlight and darkness respectively, the regression analysis suggested 83.34% and 61.31% of the total variation in both the sunlight and dark data sets respectively can be explained by the regression models *(Table 21)*. Just as the graph shows a steady decline in both data sets, the t-test showed there are no significant differences between the two data sets *(Table 23)*. Additionally, a comparison between the summer and winter data shows that the decrease in OD is much more significant in the summer compared to winter which can be seen in both the graphical representation *(Fig:4.19p)* and the t-test *(Table:24)*.

5.2.4 *Vibrio WT324*: According to data collected from phases 1 and 3, planktonic bacterial cell count was observed to increase in both data sets, sunlight and darkness exposure. In phase 1, the graphical representation showed a significant increase in cell count in the later 6 hours compared to the first 6 hours for the dark data set. For the sunlight exposed data set, a steady increase the first 6 hours was followed by a steady decline in the next 6 hours (*Fig: 4.5*). In phase 3, the graphical representation indicated the cell count remained almost constant or slight increase in the sunlight exposed data set. For the dark data set, the first 6 hours cell count remained almost constant but significantly increased in the later 6 hours *(Fig:4.14)*. A correlation analysis suggested

a moderate to strong positive correlation in phase 1 and a strong positive correlation between cell count and exposure time in phase 3. Additionally, the regression analyses suggested 46.07% and 99.33% of total variation in sunlight data set in phase 1 and phase 3 data respectively, and 88.92% and 76.73% of total variation in dark data set from phase 1 and phase 3 respectively can be explained by the regression models *(Table 5 and Table 17)*. Regardless of the graphical representation, t-test showed there are no significant differences between the two data sets *(Table 6 and Table 18)*. On the other hand, phase 2 data shows an increase in the OD of coomassie stains that were used to stain the biofilm rings post-exposure in both data sets. In the sunlight exposed data set, the graphical representation shows a steady increase up to 12 hours, and then a steady decline in the next 6 hours. The darkness exposed data set showed a similar trend except a slight decrease observed in the first 6 hours *(Fig: 4.9)*. Thus, the data indicates the biofilm rings got thicker with exposure time in both data sets, as the final OD is greater than the initial OD. This pattern shown through the graphical representation is also visible in the correlation analysis which suggested a moderate positive correlation between OD and exposure time for both data sets. Additionally, the regression analysis suggested 39.83% of total variation in the sunlight data set and 16.28% in the dark data set can be explained by the regression models *(Table 12)*. Similar to the graphical representation, t-test showed there are no significant differences between the two data sets *(Table 13)*. Finally, phase 4 showed an overall decrease in the OD of biofilms formed in an ELISA plate and exposed to sunlight and darkness. According to the graphical representation, the OD of the dark data set declined from the start whereas the OD for the sunlight exposed data set increased in the first 6 hours, and then declined sharply in the next 4 hours. This was followed by an increase in the next 2 hours, and a final steady decline in the last 6 hours. For both data sets, the sharpest decline was during 6-10 hours of exposure time. In the dark data set, the OD was found to slightly increase during 4-6 hours and during 10-12 hours. In both data sets, the OD declined to almost the same value in the 18th hour *(Fig: 4.18)*. The correlation analysis showed a strong to moderate negative correlation between OD of biofilms and exposure time in sunlight and darkness respectively, the regression analysis suggested 75.60% and 41.94% of the total variation in both the sunlight and dark data sets respectively can be explained by the regression models *(Table 22)*. Just as the graph shows a steady decline in both data sets, the t-test showed there are no significant differences between the two data sets *(Table 23)*. Additionally, a comparison between the summer and winter data shows that the decrease in OD is much more significant in

the summer compared to winter which can be seen in both the graphical representation *(Fig:4.19n)* and the t-test *(Table:24)*.

5.3 Limitations

In this experiment, only 4 strains of bacteria were used to determine the effects of winter sunlight and darkness on bacterial biofilm. The study could have included more strains of bacteria, especially of *Vibrio Cholerae* to obtain a more generalized result. In addition, the bacterial strains were grown in LB media for this experiment. Unless other media are used to find similar results, it can be difficult to confirm the effects of sunlight on the biofilm. Besides, after 6 hours, a second biofilm ring was observed to form in phase 1, which was not addressed in this study.

Moreover, three to five weeks of data were obtained for every phase of the experiment. For every phase of the experiment, more raw data should have been collected. Furthermore, this study looks into the effect of winter sunlight on the bacterial biofilm, however, other factors other than the sunlight could also have an effect on the biofilm. Although similar conditions were maintained for both sets- sunlight and dark, the study does not completely rule out the effects of other factors.

In Bangladesh, cholera outbreaks occur in two different seasons. This study was conducted from December to March, and the previous summer study was conducted from March to June. So, study is not conducted for a few months. If the data for those months are also included, a broader picture could be derived.

5.4 Future Prospect of the Research

Previously, data was collected for this study in summer, and this study collected data in winter. Thus, data for a year has been collected. Now, the experiment has to be continued for at least another year, to derive a conclusive result.

5.5 Future research

This study looks into the effect of sunlight on biofilm. This leaves a scope of further research to find which component of the sunlight actually affects the biofilm. Moreover, what triggers the biofilm resuscitation in summer and why that mechanism is not that effective in winter can be further investigated. This study primarily focuses on the effect of winter sunlight on the biofilm produced by *Vibrio Cholerae*. The effect of sunlight on biofilm produced by other seasonal pathogens can also be further investigated.

Chapter 6:

Conclusion

6.0 Conclusion

To sum it up, the study was conducted to analyze the effects of winter sunlight on bacterial biofilm produced by bacteria causing seasonal epidemics. In summer, frequent cholera and diarrhea outbreaks occur; however, these diseases are not that prevalent in winter. Sunlight could be a major factor resuscitating biofilm in summer causing these seasonal epidemics. In our study, the results suggested winter sunlight does not cause a significant breakage of bacterial biofilm. When the same study was conducted in summer, a huge difference was observed. Thus, the results indicate that even though summer sunlight can resuscitate bacterial biofilm, winter sunlight does not significantly break bacterial biofilm. Therefore, it can be said that cholera and diarrhea decreases in the winter as sunlight does not break the biofilm to release the infectious planktonic bacteria into the environment. However, more seasonal data is required to conclusively confirm this statement.

Chapter 7:

References

7.0 References

Alam, M., Sultana, M., Nair, G., Siddique, A., Hasan, N., & Sack, R. et al. (2007). Viable but nonculturable Vibrio cholerae O1 in biofilms in the aquatic environment and their role in cholera transmission. Proceedings Of The National Academy Of Sciences, 104(45), 17801-17806.

Baker-Austin, C., Oliver, J. D., Alam, M., Ali, A., Waldor, M. K., Qadri, F., & Martinez-Urtaza, J. (2018). Vibrio spp. infections. Nature Reviews Disease Primers, 4(1), 1-19.

Berk, V., Fong, J. C., Dempsey, G. T., Develioglu, O. N., Zhuang, X., Liphardt, J., & Chu, S. (2012). Molecular architecture and assembly principles of Vibrio cholerae biofilms. Science, 337(6091), 236-239.

Bridges, A. A., & Bassler, B. L. (2019). The intragenus and interspecies quorum-sensing autoinducers exert distinct control over Vibrio cholerae biofilm formation and dispersal. PLoS biology, 17(11), e3000429.

Del Pozo, J. (2017). Biofilm-related disease. Expert Review Of Anti-Infective Therapy, 16(1), 51-65.

Dhaka Wasa must answer for cholera outbreak. The Daily Star. (2022). Retrieved 12 May 2022, from https://www.thedailystar.net/views/editorial/news/dhaka-wasa-must-answer-cholera-outbreak-2993291.

Dong, C., Beis, K., Nesper, J., Brunkan, A. L., Clarke, B. R., Whitfield, C., & Naismith, J. H. (2006). The structure of Wza, the translocon for group 1 capsular polysaccharides in Escherichia coli, identifies a new class of outer membrane protein. Nature, 444(7116), 226.

E. coli. Who.int. (2018). Retrieved 3 June 2022, from https://www.who.int/news-room/fact-sheets/detail/e-coli.

Faruque, S., Naser, I., Islam, M., Faruque, A., Ghosh, A., & Nair, G. et al. (2005). Seasonal epidemics of cholera inversely correlate with the prevalence of environmental cholera phages. Proceedings Of The National Academy Of Sciences, 102(5), 1702-1707.

Fong, J. C., Syed, K. A., Klose, K. E., & Yildiz, F. H. (2010). Role of Vibrio polysaccharide (vps) genes in VPS production, biofilm formation and Vibrio cholerae pathogenesis. Microbiology, 156(Pt 9), 2757.

Fong, J. N., & Yildiz, F. H. (2015). Biofilm matrix proteins. Microbiology spectrum, 3(2), 3-2.

Hall-Stoodley, L., & Stoodley, P. (2005). Biofilm formation and dispersal and the transmission of human pathogens. Trends in microbiology, 13(1), 7-10.

Hammer, B. K., & Bassler, B. L. (2003). Quorum sensing controls biofilm formation in Vibrio cholerae. Molecular microbiology, 50(1), 101-104.

Hollmann, B., Perkins, M., & Walsh, D. (2014). Biofilms and their role in pathogenesis. British Society for Immunology. Available online: https://www.immunology.org/public-information/bitesized-immunology/pathogens-andd%20sease/biofilms-and-their-role-in (accessed on 7 August 2020).

Huq, A., Whitehouse, C. A., Grim, C. J., Alam, M., & Colwell, R. R. (2008). Biofilms in water, its role and impact in human disease transmission. Current Opinion in Biotechnology, 19(3), 244-247.

Karpman, D. (2012). Management of Shiga toxin-associated Escherichia coli-induced haemolytic uraemic syndrome: randomized clinical trials are needed. Nephrology Dialysis Transplantation, 27(10), 3669-3674.

Lequin, R. M. (2005). Enzyme immunoassay (EIA)/enzyme-linked immunosorbent assay (ELISA). Clinical chemistry, 51(12), 2415-2418.

Li, J., Attila, C., Wang, L., Wood, T. K., Valdes, J. J., & Bentley, W. E. (2007). Quorum sensing in Escherichia coli is signaled by AI-2/LsrR: effects on small RNA and biofilm architecture. Journal of bacteriology, 189(16), 6011-6020.

LSR - Lipolysis-stimulated lipoprotein receptor - Homo sapiens (Human) - LSR gene & protein. Uniprot.org. (2006). Retrieved 3 June 2022, from https://www.uniprot.org/uniprot/Q86X29.

Mosharraf, F. B., Chowdhury, S. S., Ahmed, A., & Hossain, M. M. (2020). A Comparative Study of Static Biofilm Formation and Antibiotic Resistant Pattern between

Environmental and Clinical Isolate of Pseudomonas aeruginosa. Advances in Microbiology, 10(12), 663-672.

Naser, I. B., Hoque, M. M., Abdullah, A., Bari, S. N., Ghosh, A. N., & Faruque, S. M. (2017). Environmental bacteriophages active on biofilms and planktonic forms of toxigenic Vibrio cholerae: Potential relevance in cholera epidemiology. *PLoS One*, *12*(7), e0180838.

Nastasijevic, I., Schmidt, J. W., Boskovic, M., Glisic, M., Kalchayanand, N., Shackelford, S. D., & Bosilevac, J. M. (2020). Seasonal prevalence of Shiga toxin-producing Escherichia coli on pork carcasses for three steps of the harvest process at two commercial processing plants in the United States. Applied and environmental microbiology, 87(1), e01711-20.

Pena, R. T., Blasco, L., Ambroa, A., González-Pedrajo, B., Fernández-García, L., López, M., & Tomás, M. (2019). Relationship between quorum sensing and secretion systems. Frontiers in Microbiology, 10, 1100.

Preda, V. G., & Săndulescu, O. (2019). Communication is the key: biofilms, quorum sensing, formation and prevention. Discoveries, 7(3).

Rodger, A., & Sanders, K. (2017). UV-visible absorption spectroscopy, biomacromolecular applications. In Encyclopedia of spectroscopy and spectrometry (pp. 495-502). Elsevier.

Silva, A. J., & Benitez, J. A. (2016). Vibrio cholerae biofilms and cholera pathogenesis. PLoS neglected tropical diseases, 10(2), e0004330.

Steinberg, T. H. (2009). Protein gel staining methods: an introduction and overview. Methods in enzymology, 463, 541-563.

Stepanović, S., Vuković, D., Dakić, I., Savić, B., & Švabić-Vlahović, M. (2000). A modified microtiter-plate test for quantification of staphylococcal biofilm formation. Journal Of Microbiological Methods, 40(2), 175-179.

Sultana, M., Nusrin, S., Hasan, N., Sadique, A., Ahmed, K., & Islam, A. et al. (2018). Biofilms Comprise a Component of the Annual Cycle of Vibrio cholerae in the Bay of Bengal Estuary. Mbio, 9(2).

Van Houdt, R., & Michiels, C. W. (2005). Role of bacterial cell surface structures in Escherichia coli biofilm formation. Research in microbiology, 156(5-6), 626-633.

Vogeleer, P., Tremblay, Y. D., Mafu, A. A., Jacques, M., & Harel, J. (2014). Life on the outside: role of biofilms in environmental persistence of Shiga-toxin producing Escherichia coli. Frontiers in microbiology, 5, 317.